Journal of Quantitative Spectroscopy & Radiative Transfer 202 (2017) 286–301

Contents lists available at ScienceDirect

Journal of Quantitative Spectroscopy & Radiative Transfer

journal homepage: www.elsevier.com/locate/jqsrt

Radiative transition probabilities for the main diatomic electronic systems of N_2, N_2^+, NO, O_2, CO, CO^+, CN, C_2 and H_2 produced in plasma of atmospheric entry

Z. Qin[a], J.M. Zhao[a], L.H. Liu[a,b,*]

[a] School of Energy Science and Engineering, Harbin Institute of Technology, Harbin 150001, China
[b] Department of Physics, Harbin Institute of Technology, Harbin 150001, China

ARTICLE INFO

Article history:
Received 28 April 2017
Revised 2 August 2017
Accepted 9 August 2017
Available online 18 August 2017

Keywords:
Radiative transition probabilities
Radiative lifetimes
Diatomic molecules
N_2–O_2
CO_2–N_2
H_2

ABSTRACT

Accurate radiative transition probabilities of diatomic electronic systems are required to calculate the discrete radiation of plasmas. However, most of the published transition probabilities are obtained using older spectroscopic constants and electronic transition moment functions (ETMFs), some of which deviates greatly from experimental data. Fortunately, a lot of new spectroscopic constants that include more anharmonic correction terms than the earlier ones have been published over the past few years. In this work, the Einstein coefficients, Franck–Condon factors and absorption band oscillator strengths are calculated for important diatomic radiative transition processes of N_2-O_2, CO_2-N_2 and H_2 plasmas produced in entering into the atmosphere of Earth, Mars and Jupiter. The most up-to-date spectroscopic constants are selected to reconstruct the potential energy curves by the Rydberg–Klein–Rees (RKR) method. Then the vibrational wave functions are calculated through the resolution of the radial Schrödinger equation for such potential energy curves. These results, together with the latest "ab-initio" ETMFs derived from the literature are used to compute the square of electronic-vibrational transition moments, Einstein coefficients and absorption band oscillator strengths. Moreover, the Franck–Condon factors are determined with the obtained vibrational wave functions. In the supplementary material we present tables of the radiative transition probabilities for 40 band systems of N_2, N_2^+, NO, O_2, CO, CO^+, CN, C_2 and H_2 molecules. In addition, the calculated radiative lifetimes are systematically validated by available experimental results.

© 2017 Elsevier Ltd. All rights reserved.

1. Introduction

Accurate radiative transition probabilities are key to scientific research areas including plasma optical diagnostics [1,2], quantitative spectroscopy [2,3], analyzation of emission from gas discharge and afterglows [4,5], radiation modeling of atmospheric entry [6–8,58], etc. In particular, strong shock waves, formed in front of the vehicles during hypersonic flights, translate part of the kinetic energy of the vehicles into internal energy of the gases. The high-temperature gases will radiate, and the emitted radiation may also contribute to the heat flux suffered by the vehicles, which will be very important for vehicles that enter into the atmosphere at very high speed. Hence, the prediction of radiation for high-temperature gases in shock layers is required for the efficient design of thermal protection systems. The emission coefficients ε_σ of high-temperature gases is generally given by

$$\varepsilon_\sigma = \sum_{ul} \frac{A_{ul}}{4\pi} hc\nu_{ul} N_u f_{ul}(\nu - \nu_{ul}) \quad (1)$$

where A_{ul} is the Einstein coefficients N_u denotes the population of the upper transition levels. ν_{ul} is the wavenumber, and $f_{ul}(\nu - \nu_{ul})$ is the spectral line shape of the transition. Einstein coefficients, as a form of radiative transition probabilities, are vital to the determination of the emission coefficients that are utilized further to calculate the radiative heat flux.

Einstein coefficients, absorption band oscillator strength and Franck–Condon factors are three forms of the radiative transition probabilities. The first two parameters can be calculated from the square of electronic-vibrational transition moment and Franck–Condon factors are determined with the vibrational wave functions. Moreover, the square of electronic-vibrational transition moment can be calculated using Franck–Condon factors $q_{v'v''}$ (v' and v'' are vibrational levels in the upper and lower electronic levels of transition, respectively), electronic transition moment function

* Corresponding author at: School of Energy Science and Engineering, Harbin Institute of Technology, 92 West Dazhi Street, Harbin 150001, China
E-mail address: lhliu@hit.edu.cn (L.H. Liu).

http://dx.doi.org/10.1016/j.jqsrt.2017.08.010
0022-4073/© 2017 Elsevier Ltd. All rights reserved.

(ETMF) $R_e(r)$ and r-centroids $r_{v'v''}$ in the r-centroid approximation [9,10]:

$$\left(R_e^{v'v''}\right)^2 \cong [R_e(\bar{r}_{v'v''})]^2 q_{v'v''} \tag{2}$$

Such approximations often need to be combined with the limited experimental data to calculate Einstein coefficients for the large number of band systems. Another more rigorous method to obtain the square of electronic-vibrational transition moment is given by

$$\left(R_e^{v'v''}\right)^2 = \left[\int_0^\infty \psi_{v'}(r) R_e(r) \psi_{v''}(r) dr\right]^2 \tag{3}$$

where r is the internuclear distance, $\psi_{v'}(r)$ and $\psi_{v''}(r)$ are the corresponding radial vibrational wave functions and $R_e(r)$ is the ETMF, which is an average of the electric dipole moment with respect to the electronic wave function.

Thus, in order to precisely determine the electronic-vibrational transition moment, it is necessary to obtain the parameters of the vibrational wave functions and the ETMF. The vibrational wave function can be obtained by solving the radial Schrödinger equation over the potential energy curve for a selected electronic state of a molecule. And the potential energy curves of the different electronic states of a diatomic molecule can be determined by the ab-initio method [11] or the Rydberg–Klein–Rees (RKR) method [12–14]. The ab-initio method, based on quantum chemistry theory, can predict the potential energy curves to a good level of precision, whereas the RKR method, a more straightforward method grounded on experimental spectroscopic constants, can predict potential curves more accurately for internuclear distances where the spectroscopy constants are valid. Therefore, the RKR method is chosen to reconstruct the potential curves for the efficient internuclear distances in this paper. The ETMF can be determined by band strength measurements, or obtained by quantum-mechanical calculations which have been proved to attain an accuracy comparable to that of many band intensity measurements. Besides, such calculations cover a wider range of internuclear distances than those by the r-centroid approximation method [15]. For these reasons, the relation of Eq. (3) is used to calculate the electronic-vibrational transition moments taking advantage of the accurate spectroscopy constants and ab-initio ETMFs for all the band systems considered here.

In view of the important role of transition probabilities for diatomic molecular band systems of plasmas in hypersonic flights, a lot of data of transition probabilities have been published over the past few decades. Krupenie [16] gave a critical review and completion of the observed and predicted spectroscopy data of O_2 and its ions O_2^-, O_2^+ and tabulated many of these transition probabilities for several oxygen band systems. Lofthus and Krupenie [17] presented many of these transition probabilities for several band systems of N_2 and its ions N_2^-, N_2^+. Subsequently, many papers were published regarding transition probabilities for some band systems of N_2, N_2^+, O_2, NO, CO, CO^+, CN, and C_2 diatomic molecules [18–25]. More recently, da Silva and Dudeck [26] calculated Franck–Condon factors, Einstein coefficients and absorption band oscillator strengths for the most prominent diatomic radiative transitions in high-temperature CO_2–N_2 plasmas. In addition, Chauveau et al. [27] constructed a spectroscopic database for all the contributing electronic systems of air diatomic molecules based on transition probabilities, whose correctness and precision had been proved by measured radiative lifetimes. A similar approach was taken by Babou et al. [28] to obtain transition probabilities of diatomic electronic band systems for CO_2–N_2 plasma, including CO, CO^+, CN and C_2 molecules.

However, the transition probabilities are still incomplete and some of them are less accurate. Moreover, many spectroscopic constants and ETMFs are so old that can be superseded by more recent measurements and calculations. For these reasons, the potential energy curves of electronic states of N_2, N_2^+, NO, O_2, CO, CO^+, CN, C_2 and H_2 molecules have been reconstructed by RKR method starting from the selected most up-to-date spectroscopic constants. Then the vibrational wave functions are attained by solving the radial Schrödinger equation over the reconstructed energy potential curves. Finally, we calculate the transition probabilities for all the band systems considered using vibrational wavefunctions and ETMFs available in the literature. To validate the calculated transition probabilities, the vibrational radiative lifetimes calculated from Einstein coefficients are systematically compared with available experimental results and other calculations. This paper is organized as follows. In Section 2, we describe the details of the RKR method. The results of reconstructed potential energy curves are given in Section 3. In Sections 4 and 5, the results of transition probabilities and radiative lifetimes are given and discussed. In Section 6, conclusions are drawn.

2. Methods of calculation

The RKR method is a widely used first-order semiclassical inversion procedure for reconstructing potential energy curves of diatomic electronic states. This theory is extensively discussed in a number of literatures and monographs [12–14,29–30]. The key conclusions of this theory are made up of two Klein integrals, which are given by [29]

$$r_2(v) - r_1(v) = 2\sqrt{\frac{\hbar^2}{2\mu}} \int_{v_{\min}}^{v} \frac{dv'}{[G_v - G_{v'}]^{1/2}} = 2f(v) \tag{4}$$

$$\frac{1}{r_1(v)} - \frac{1}{r_2(v)} = 2\sqrt{\frac{2\mu}{\hbar^2}} \int_{v_{\min}}^{v} \frac{B_{v'} dv'}{[G_v - G_{v'}]^{1/2}} = 2g(v) \tag{5}$$

where $r_1(v)$ and $r_2(v)$ are inner and outer classical turning points of the potential curve for a given vibrational level, μ is the reduced mass of the molecule, and $\hbar$ is the reduced Planck's constant, $v_{\min}$ is the non-integer effective value of the vibrational quantum number at the potential minimum, namely the zero of vibrational level energy G_v, B_v is the inertial rotational constant for that vibrational level, and they can be expanded as

$$G_v = \sum_{l=1}^{n} Y_{l,0}(v+1/2)^l = \omega_e(v+1/2) - \omega_e\chi_e(v+1/2)^2 + \cdots \tag{6}$$

$$B_v = \sum_{l=0}^{m} Y_{l,1}(v+1/2)^l = B_e - \alpha_e(v+1/2) + \cdots \tag{7}$$

where $Y_{l,0}$ and $Y_{l,1}$ are Dunham coefficients rearranged by equilibrium spectroscopic constants that are adjusted on experimental determined vibrational energy at each vibrational quantum number v. The most accurate available spectroscopic constants that include more anharmonic correction terms are selected. The values and references of spectroscopic constants selected for each electronic state are presented in Appendix A. Rearrangement of the Eqs. (4)–(5) yields the RKR classical turning point expressions [29]:

$$r_1(v) = \sqrt{\frac{f(v)}{g(v)} + f^2(v)} - f(v) \tag{8}$$

$$r_2(v) = \sqrt{\frac{f(v)}{g(v)} + f^2(v)} + f(v) \tag{9}$$

In order to remove the singularity in the integral $f(v)$ and $g(v)$ at $v' = v$ and maintain high accuracy, the expressions of $f(v)$ and $g(v)$ have been integrated using a 128 points Gauss-type quadrature. And for the sake of calculating the vibrational wave functions, it is important to interpolate the potential energy curve between $r_1(v)$ and $r_2(v)$ and extrapolate that potential energy curve

beyond this internuclear distance. The interpolation is done with a high-order Lagrange polynomial [31]. Outside this region, the RKR potential energy curve has been extrapolated by using a repulsive function $U_{rep}(r)$ for the shorter internuclear distance and a Hulburt and Hirschfelder potential $U_{HH}(r)$ [32] for the longer internuclear distance, which can accurately give continuous single-well potential energy curve. These two functions are written as [32]

$$U_{rep}(r) = \frac{a_1}{r^{b_1}} \tag{10}$$

$$U_{HH}(r) = D_e\left[1 - e^{-a_2(r-r_e)}\right]^2 + D_e\left[b_2 a_2^3 (r-r_e)^3 e^{-2a_2(r-r_e)}(1 + a_2 c_2 (r-r_e))\right] \tag{11}$$

where D_e and r_e refer to the dissociation energy of the electronic (relative to bottom of the potential energy curve) and the equilibrium internuclear distance, respectively. a_1, b_1, a_2, b_2 and c_2 are floating parameters that need to be adjusted to ensure continuity with the potential energy curve and they are adjusted in order that each extrapolation function fits a significant part of the extremity of the reconstructed potential energy curve, too.

The reconstructed potential energy curves are utilized in radial Schrödinger equation to obtain the vibrational wave functions, and the ETMFs derived from references are summarized in Section 3. The knowledge of ETMF $R_e(r)$ and vibrational wave function $\psi_v(r)$ allows determining the transition probabilities such as Einstein coefficients $A_{v'v''}$, absorption band oscillator strengths $f^{abs}_{v'v''}$, the Franck–Condon factor $q_{v'v''}$ and radiative lifetimes $\tau_{v'}$ through the following expressions [33,34]:

$$A_{v'v''} = 2.026 \times 10^{-6} \eta^3_{v'v''} \frac{2 - \delta_{0,\Lambda'+\Lambda''}}{2 - \delta_{0,\Lambda'}} \left(R_e^{v'v''}\right)^2 \tag{12}$$

$$f^{abs}_{v'v''} = 3.0376 \times 10^{-6} \eta_{v'v''} \frac{2 - \delta_{0,\Lambda'+\Lambda''}}{2 - \delta_{0,\Lambda'}} \left(R_e^{v'v''}\right)^2 \tag{13}$$

$$q_{v'v''} = \left(\int \psi_{v'}(r)\psi_{v''}(r)dr\right)^2 \tag{14}$$

$$\tau_{v'} = \frac{1}{\sum_{v''=0}^{v''_{\max}} A_{v'v''}} \tag{15}$$

where $\eta_{v'v''}$ is the wavenumber of the vibrational band system. Λ' and Λ'' are the projections of the electronic orbital angular momentum on the internuclear axis for the upper and lower electronic levels, respectively.

3. Reconstructed potential energy curves

The most accurate and up-to-date spectroscopic constants and the dissociation limits, which are given in Appendix A, have been selected from the literature. The equilibrium internuclear distance r_e of the potential energy curve is selected from Ref. [40] when that is unavailable in the references given in Appendix A. The traditional spectroscopic constants are usually rearranged into Dunham coefficients. The relation between Dunham coefficients and traditional spectroscopic constants can be easily deduced from Eqs. (6)–(7). Note that $v^{\max}$ is the maximum v value of experimental measurements to adjust the potential energy curve for the extrapolations described in Eqs. (10)–(11). Namely, $v^{\max}$ is the maximum vibrational level where the Dunham coefficients are valid. Based on accurate spectroscopic constants, the reconstructed potential energy curves can be obtained by the method elaborated in Section 2. The resulting potential energy curves are potted in Fig. 1 for the 44 electronic states involved in the radiative transitions in Table 1. Furthermore, for some states, the extrapolation regions are strongly perturbed so that such extrapolations are questionable. The notations of these states are marked in red and italics in Fig.1 and the corresponding potential energy curves always show peak values.

The ETMFs for each electronic transition system are obtained from references given in Table 1. For most of the electronic transition systems, we select the “ab-initio” ETMFs to calculate the radiative transition probabilities. Some of the ETMFs determined by experiments are selected when the corresponding “ab-initio” ETMFs are not available in the literature. Details of the selected ETMFs are given in Section 5.

4. Radiative transition probabilities

Tables of radiative transition probabilities (Einstein coefficients, absorption band oscillator strengths and Franck–Condon factors) have been given in supplementary material for each electronic transition system of N_2, N_2^+, NO, O_2, CO, CO^+, CN, C_2 and H_2 diatomic molecules.

5. Vibrational radiative lifetimes

Details of the selected ETMFs for different electronic transition systems of N_2, N_2^+, NO, O_2, CO, CO^+, CN, C_2 and H_2 diatomic molecules and comparisons with the theoretical and experimental radiative lifetimes in the literature are given in this section. For most of electronic transition systems, our calculated results are in good agreement with the available experimental results.

5.1. N_2 transitions

For the First-positive system, Chauveau et al. [27] calculated two vibrational radiative lifetimes with the ETMFs in Refs. [63,145] and gave a list of experimental results from various references. We select the latest ab-initio ETMF of Ref. [172] to obtain radiative transition probabilities, from which the vibrational radiative lifetimes of the $B^3\Pi_g$ electronic state of N_2 are calculated and shown in Fig. 2(a). Fig. 2(a) also shows different theoretical and experimental results from the references. Most of the experimental results are distributed between two calculated vibrational radiative lifetimes from Chauveau et al. [27]. Our calculated results are approximately the mean of these two results and are in good agreement with the experimental results, especially with the latest ones from [91].

For the Second-positive system, we choose the ETMF in Ref. [63]. Fig. 2(b) gives the various theoretical and experimental vibrational radiative lifetimes of the $C^3\Pi_u$ electronic state of N_2. The experimental radiative lifetimes scatter to a large extent and have a larger range of error. Our calculated results are within the allowable error range of the experimental results except for $v' = 4$. Radiative lifetimes from Ref. [27] are also plotted in Fig. 2(b) and these values are smaller than the present results, although they have been obtained from the same ETMF.

Concerning Vegard–Kaplan system, we select the ETMF of Ref. [87] as recommended and reported by Gilmore et al. [24]. The Einstein coefficients calculated in this work are in very good agreement with the results obtained by Gilmore et al. [15]. Spectroscopic observations have provided firm evidence for the 1.36±0.27 s lifetime of the $\Sigma = 0$ sub-state of $A^3\Sigma_u^+$ by Shemansky and Carleton [88]. The present calculated radiative lifetime is 1.63 s, which is very close to the value observed by Shemansky and Carleton for the level $v' = 0$ of the $A^3\Sigma_u^+$ electronic state.

The ETMFs selected for the Wu–Benesch, Lyman–Birge–Hopfield and IR afterglow systems are from Ref. [24], which give the ETMFs

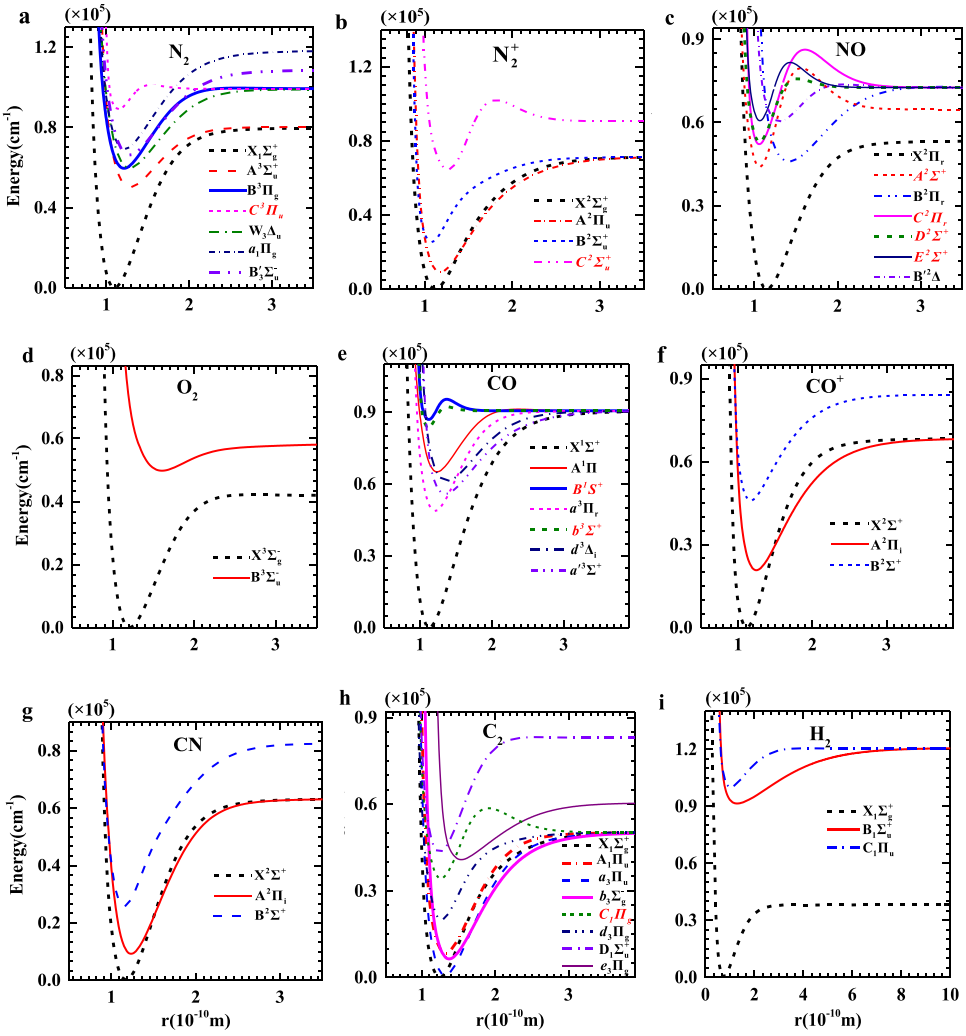

Fig. 1. Reconstructed potential energy curves of the selected electronic states of **(a)** N_2, **(b)** N_2^+, **(c)** NO, **(d)** O_2, **(e)** CO, **(f)** CO^+, **(g)** CN, **(h)** C_2 and **(i)** H_2 molecules.

by fitting theoretical values or geometric mean of theoretical results from previous literatures. In the case of Wu–Benesch system, Fig. 2(c) shows the vibrational radiative lifetimes of the $W^3\Delta_u$ electronic state of N_2 from this work and other references. A good agreement has been achieved between our results and the calculated results from Werner et al. [39] and Gilmore et al. [15]. With respect to Lyman–Birge–Hopfield system, a quite good agreement is observed in Fig. 2(d) between our results and the theoretical results of Ref. [101], but a deviation of about 4% is observed at $v' = 1$ between the present radiative lifetime and the one measured by Marinelli et al. [102]. As for IR afterglow system, it is difficult to find the experimental radiative lifetimes of the $B'^3\Sigma_u$ electronic state of N_2, while the agreement between the present results and the calculated ones from Ref. [39] is within 5% for $v' = 0-12$.

5.2. N_2^+ transitions

For the Meinel system, we choose the ETMF published by Langhoff et al. [66], and a very good agreement with the experimental radiative lifetimes from Ref. [104–106] is acquired, although the present radiative lifetimes are slightly larger than the calculated ones of Ref. [27], just as shown in Fig. 3(a).

Considering the First-negative and Second-negative systems, the ETMFs of Ref. [67] are used in this paper. We have plotted in Fig. 3(b) and (c) the present radiative lifetimes, theoretical radiative lifetimes from Ref. [27] and other two experimental values of the $B^2\Sigma_u^+$ electronic state and the $C^2\Sigma_u^+$ electronic state of N_2^+. A larger value of radiative lifetimes are observed compared to that of Ref. [27], but our results are closer to the experimental results.

5.3. NO transitions

Fig. 4(a) shows vibrational radiative lifetimes of the $A^2\Sigma^+$ electronic state of NO. The present calculated radiative lifetimes, which are obtained from the ETMF of Ref. [68], are in very good agreement with the calculated ones reported in Ref. [27]. The experimental results are relatively scattered, whereas our calculated results are in good agreement with the experimental results for $v' \leq 2$.

In the same way as it has been used above, we have reported in Fig. 4(b) radiative lifetimes of the $B^2\Pi_r$ electronic state of NO calculated in the present work from the ETMF of Ref. [69]. They are compared with the theoretical results of Ref. [27] and different experimental results from Refs. [89,109,114–116]. Our calculated radiative lifetimes are closer to the experimental results of Gadd and Slanger [115].

For the $C^2\Pi_r$ electronic state of NO, Brzozowski et al. [89] found the radiative lifetime of $C^2\Pi_r$ state ($v' = 0, J < 4.5$) is 32.0 ± 2.0 ns. While Smith and Read [90] obtained an upper limit of radiative lifetime of $C^2\Pi_r$ state ($v' = 0$), which is $\tau \leq 2.7\ ns$ (standard deviation 1.5 ns). What's more, the levels located higher than $v' = 0$ and

Table 1
Electronic systems for which the transition probabilities have been calculated.

Molecule	Electronic system	Upper-lower states	Calculated band ($0{:}v'_{max}$,$0{:}v''_{max}$)	Selected ETMF
N_2	First-positive	$B^3\Pi_g - A^3\Sigma_u^+$	(0:21,0:21)	[172]
	Second-positive	$C^3\Pi_u - B^3\Pi_g$	(0:4,0:21)	[63]
	Vegard–Kaplan	$A^3\Sigma_u^+ - X^1\Sigma_g^+$	(0:21,0:21)	[24]
	Wu–Benesch	$W^3\Delta_u - B^3\Pi_g$	(0:21,0:17)	[24]
	Lyman–Birge–Hopfield	$a^1\Pi_g - X^1\Sigma_g^+$	(0:21,0:21)	[24]
	IR afterglow	$B'^3\Sigma_u - B^3\Pi_g$	(0:21,0:21)	[24]
O_2	Schumann–Runge	$B^3\Sigma_u^- - X^3\Sigma_g^-$	(0:27,0:27)	[64,65]
N_2^+	Meinel	$A^2\Pi_u - X^2\Sigma_g^+$	(0:27,0:27)	[66]
	First-negative	$B^2\Sigma_u^- - X^2\Sigma_g^+$	(0:8,0:21)	[67]
	Second-negative	$C^2\Sigma_u^+ - X^2\Sigma_g^+$	(0:6,0:21)	[67]
NO	γ	$A^2\Sigma^+$-$X^2\Pi_r$	(0:12,0:22)	[68]
	β	$B^2\Pi_r$-$X^2\Pi_r$	(0:37,0:22)	[69]
	δ	$C^2\Pi_r$-$X^2\Pi_r$	(0:8,0:22)	[70]
	ε	$D^2\Sigma^+$-$X^2\Pi_r$	(0:9,0:22)	[71]
	γ'	$E^2\Sigma^+$-$X^2\Pi_r$	(0:4,0:22)	[72]
	β'	$B'^2\Delta$-$X^2\Pi_r$	(0:11,0:22)	[72]
	11,000 Å	$D^2\Sigma^+$-$A^2\Sigma^+$	(0:8,0:8)	[71]
	Infrared	$X^2\Pi_r$-$X^2\Pi_r$	(0:22,0:22)	[73]
CO	Infrared	$X^1\Sigma^+$-$X^1\Sigma^+$	(0:50,0:50)	[74]
	Fourth-positive	$A^1\Pi$-$X^1\Sigma^+$	(0:22,0:50)	[75]
	Hopfield–Birge	$B^1\Sigma^+$-$X^1\Sigma^+$	(0:1,0:50)	[77]
	Third-positive	$b^3\Sigma^+$-$a^3\Pi_r$	(0:2,0:18)	[78]
	Triplet	$d^3\Delta_i$-$a^3\Pi_r$	(0:20,0:20)	[79]
	Asundi	$a'^3\Sigma^+$-$a^3\Pi_r$	(0:20,0:18)	[80]
	Angström	$B^1\Sigma^+$-$A^1\Pi$	(0:1,0:21)	[77]
CO^+	Comet–Tail	$A^2\Pi_i$-$X^2\Sigma^+$	(0:38,0:38)	[81]
	Baldet–Johnson	$B^2\Sigma^+$-$A^2\Pi_i$	(0:50,0:50)	[81]
	First-negative	$B^2\Sigma^+$-$X^2\Sigma^+$	(0:25,0:35)	[81]
CN	Red	$A^2\Pi_i$-$X^2\Sigma^+$	(0:38,0:38)	[171]
	Violet	$B^2\Sigma^+$-$X^2\Sigma^+$	(0:27,0:36)	[82]
	LeBlanc	$B^2\Sigma^+$-$A^2\Pi_i$	(0:25,0:38)	[171]
C_2	Philips	$A^1\Pi_u - X^1\Sigma_g^+$	(0:35,0:21)	[83]
	Mulliken	$\mathbf{D}^1\Sigma_u^+ - X^1\Sigma_g^+$	(0:22,0:21)	[84]
	Deslandres–D'Azambuja	$\mathbf{C}^1\Pi_g$-$A^1\Pi_u$	(0:9,0:32)	[85]
	Ballik and Ramsay	$b^3\Sigma_g^- - a^3\Pi_u$	(0:43,0:43)	[83]
	Swan	$d^3\Pi_g$-$a^3\Pi_u$	(0:22,0:33)	[83]
	Fox–Herzberg	$e^3\Pi_g$-$a^3\Pi_u$	(0:35,0:35)	[85]
	dc	$d^3\Pi_g - c^3\Sigma_u^+$	(0:13,0:17)	[83]
H_2	Lyman	$B^1\Sigma_u^+ - X^1\Sigma_g^+$	(0:36,0:36)	[86]
	Werner	$C^1\Pi_u - X^1\Sigma_g^+$	(0:12,0:22)	[86]

$J = 4.5$ are strongly predissociated, leading to shorter radiative lifetimes of $C^2\Pi_r$ state ($v' > 0$). So we don't present comparison with the experimental results. The ETMF selected for δ system is that of Ref. [70].

Concerning the $D^2\Sigma^+$ electronic state of NO, both the ε system and 11,000 Å system contribute to the vibrational radiative lifetimes of NO $D^2\Sigma^+$ electronic state. The radiative lifetimes calculated from the ETMF of Ref. [71] are larger (about 5–18%) than the calculated ones of Ref. [27], although they use the same ETMF. Our calculated results are within the error bars of experimental results for $v' = 0$, 3, as shown in Fig. 4(c).

As to the $B'^2\Delta$ electronic state of NO, Fig. 4(d) shows the radiative lifetimes of vibrational levels of the present results, the theoretical values of Ref. [27] and various experimental results of Refs. [89, 118–120]. The ETMF of Ref. [72] has been used in this paper. The different experimental radiative lifetimes are distributed desultorily and our calculated results are bounded by these experimental results.

The infrared system of NO greatly contributes to the discrete radiation of the N_2–O_2 plasma in the infrared region and has been studied thoroughly in the literature. We select the ETMF of Ref. [73] to calculate the Einstein coefficients that agree well (about 1.5%) with the calculated ones of Ref. [27]. Compared to the experimental results [146–151], a deviation of about 9% is observed at (v', v'') = (1, 0). It should be also noted that a deviation is about 4% in comparison with the experimental results [146,147] at (v', v'') = (2, 0).

On the whole, although experimental radiative lifetimes of the NO $A^2\Sigma^+$, $B^2\Pi_r$, $D^2\Sigma^+$, $B'^2\Delta$ electronic states exhibit a quite large dispersion, our calculated results are bounded by these experimental data.

5.4. O_2 transitions

For O_2 Schumann–Runge band, the ETMF of Ref. [64], shifted by -0.049 a_0 as suggested by Friedman [65], is used in this work with the extrapolations of the ETMF from Ref. [65]. As shown in Fig. 5, the absorption oscillator strengths obtained using this ETMF are slightly lower than the calculations of Chauveau et al. [27], whereas the results are between the experimental results from Ref. [121] and Ref. [122] for $v' = 0-19, v'' = 0$, and they are closer to the experimental results [122] for $v' = 0-19, v'' = 1$.

5.5. CO transitions

Due to the great contribution to the discrete radiation of the CO_2–N_2 plasma in the VUV region, the Fourth-positive system of CO have been widely investigated, and different ETMFs have been given in the past few years. Field et al. [123] obtained this ETMF by

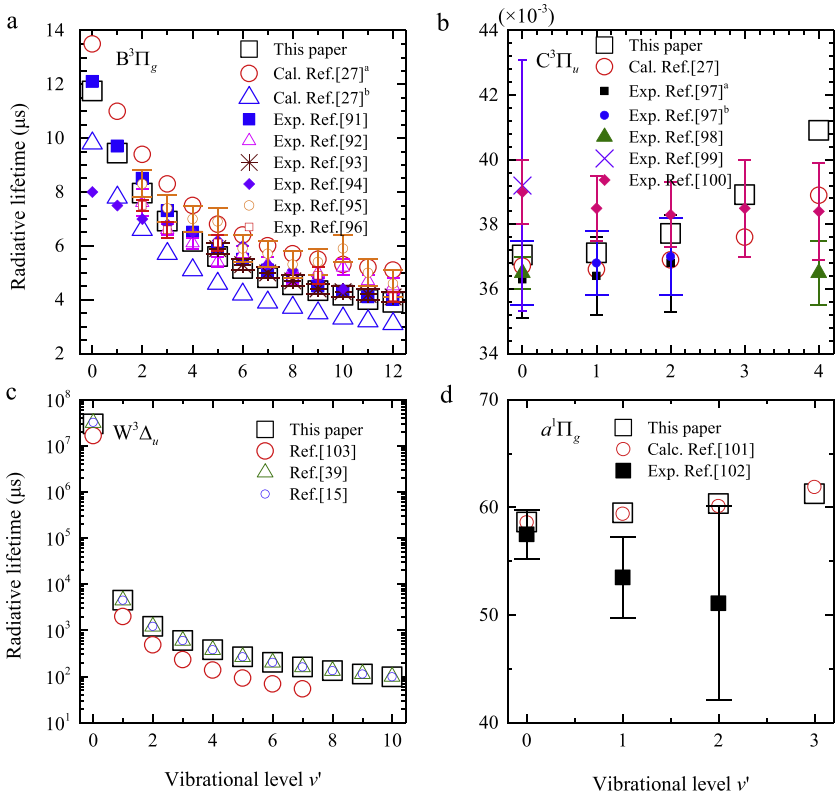

Fig. 2. Comparison of the vibrational radiative lifetimes calculated in the present work for N_2, **(a)** $B^3\Pi_g$ electronic state with the results of Refs. [27]a (calculation with ETMF of Ref. [63]), [27]b (calculation with ETMF of Ref. [145]), [91–96], **(b)** $C^3\Pi_u$ electronic state with the results of Refs. [27], [97]a (Phase-shift method), [97]b (Delayed-coincidence method), [98–100], **(c)** $W^3\Delta_u$ electronic state with the results of Refs. [103,39,15], **(d)** $a^1\Pi_g$ electronic state with the results of Refs. [101-102].

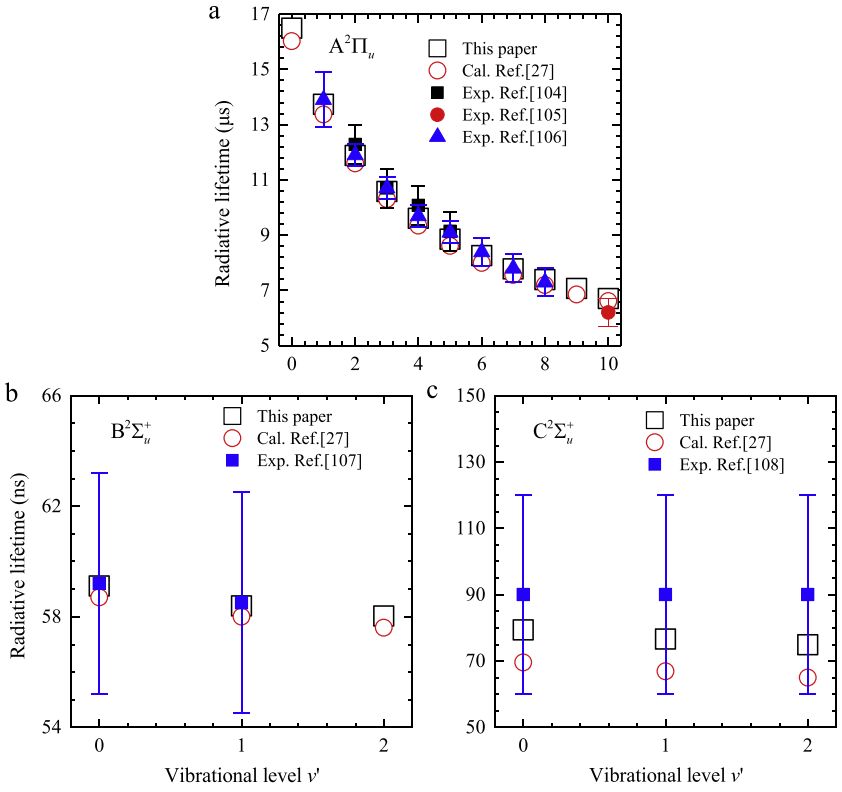

Fig. 3. Comparison of the vibrational radiative lifetimes calculated in the present work for N_2^+, **(a)** $A^2\Pi_u$ electronic state with the results of Refs. [27,104–106], **(b)** $B^2\Sigma_u^+$ electronic state with the results of Refs. [27,107], **(c)** $C^2\Sigma_u^+$ electronic state with the results of Refs. [27,108].

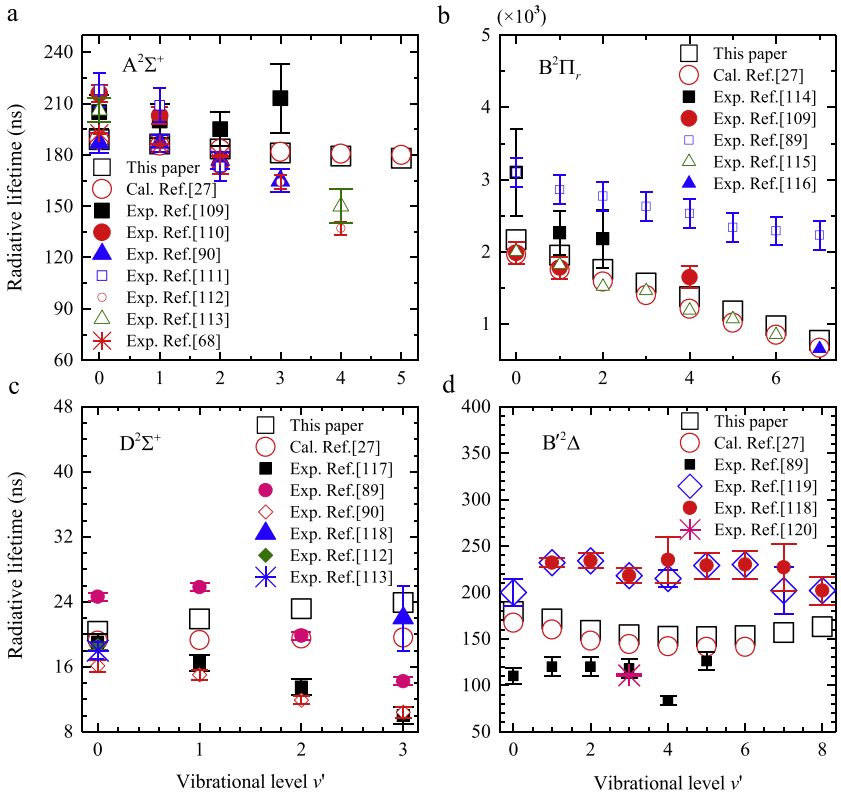

Fig. 4. Comparison of the vibrational radiative lifetimes calculated in the present work for NO, **(a)** $A^2\Sigma^+$ electronic state with the results of Refs. [27,68,90,109–113], **(b)** $B^2\Pi_r$ electronic state with the results of Refs. [27,89,109,114–116], **(c)** $D^2\Sigma^+$ electronic state with the results of Refs. [27,89–90,112–113,117–118], **(d)** $B'^2\Delta$ electronic state with the results of Refs. [27,89,118–120].

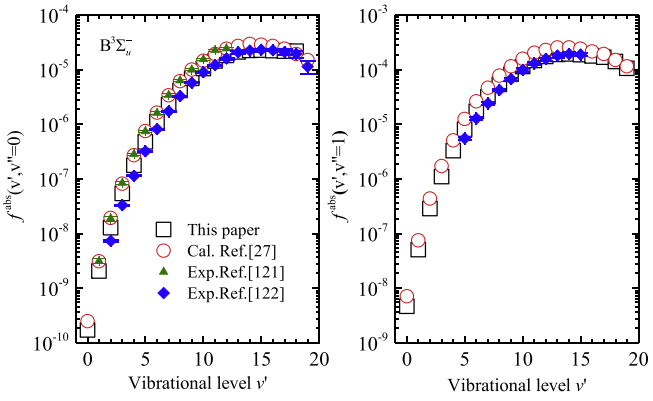

Fig. 5. Comparison of absorption oscillator strengths calculated in the present work for O_2 Schumann–Runge band with the results of Refs. [27,121,122]

measuring radiative lifetimes using synchrotron radiation. DeLeon [75,76] deduced the ETMF by using the laser induced fluorescence. And Kirby and Cooper [77] calculated this value through the "ab-initio" method. We select the ETMF of DeLeon which enables to obtain a good agreement with the experimental radiative lifetimes of Ref. [123], just as shown in Fig. 6(a). The calculated radiative lifetimes are relatively dispersed, but the present results are among other calculated values.

For the Third-positive system, there is no "ab-initio" ETMFs for us to use in the references that we can find. Hence, we adopt the fitting formula from Ref. [26] obtained from experimental lifetimes of Carlson [78]. Table 2 shows the vibrational radiative lifetimes of the $b^3\Sigma^+$ electronic state. The radiative lifetimes obtained using

Table 2
Vibrational radiative lifetimes of the $b^3\Sigma^+$ electronic state of CO: comparison with the experimental results.

	This work	Experimental results		
		Ref. [152]	Ref. [124]	Ref. [78]
$v'=0$	57.8	57.6±1.24	56±1	53.7±1.5
$v'=1$	62.6		56±1	64.6±2

this ETMF are in good agreement with the experimental results of Ref. [152] for $v'=0$, and they are closer to the experimental data of Ref. [78] for $v'=1$.

For the Triplet system, the only ETMF that we can find is from Ref. [79], and the ETMF was calculated from the only equation in Ref. [79] using the measured radiative lifetimes, concluding with a constant of $Re=1.65$ Debye.

Considering the Asundi system, we select the ETMF of Peterson and Woods [80] that are calculated with CASSCF wave functions rather than with CI-SD wave functions since it covers a large valid range of internuclear distance. The calculated radiative lifetimes are shown in Fig. 6(b) and a good agreement with calculations of da Silva and Dudeck [26] is observed. However, our calculated results are quite larger than the only experimental radiative lifetimes of Ref. [124] we can find in the literature. The deviation decreases from 23% for $v'=4$ to 11% for $v'=9$ with the increasing v' value.

Table 3 gives the vibrational radiative lifetimes of $B^1\Sigma^+$ electronic state with comparison to the theoretical and experimental results. Both the Hopfield–Birge system and Angström system are taken into consideration here, and the ETMFs of Ref. [77] are used for these two electronic transition systems. By comparison, a good

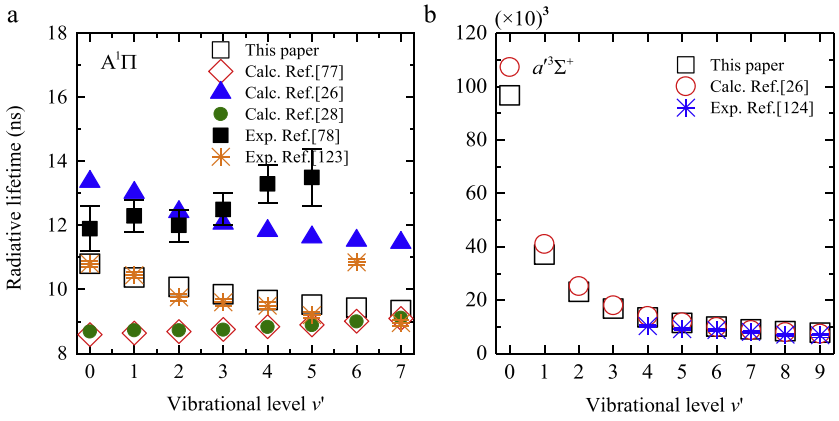

Fig. 6. Comparison of the vibrational radiative lifetimes calculated in the present work for CO, **(a)** $A^1\Pi$ electronic state with the results of Refs. [26,28,77–78,123], **(b)** $a'^3\Sigma^+$ electronic state with the results of Refs. [26,124].

Table 3
Vibrational radiative lifetimes of the $B^1\Sigma^+$ electronic state of CO: comparison with the theoretical and experimental results.

	This work	Theoretical results Ref. [77]	Experimental results Ref. [153]
$v'=0$	32.5	33.5	24.3±1.8
$v'=1$	29.4	29.2	23.8±1.4

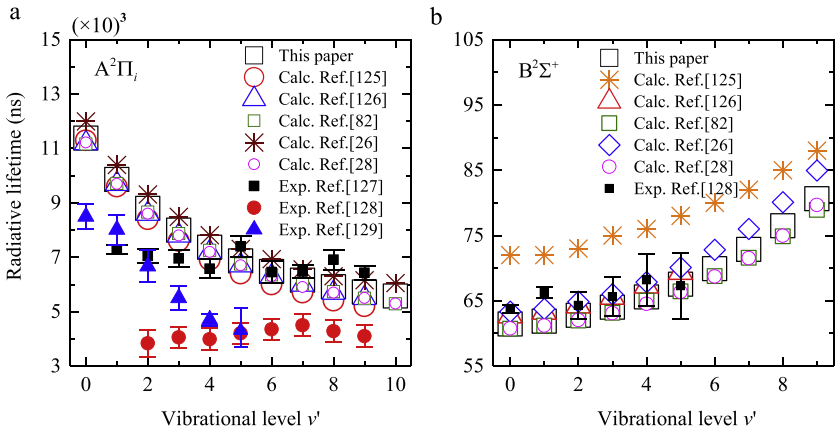

Fig. 7. Comparison of the vibrational radiative lifetimes calculated in the present work for CN, **(a)** $A^2\Pi_i$ electronic state with the results of Refs. [26,28,82,125–129], **(b)** $B^2\Sigma^+$ electronic state with the results of Refs. [26,28,82,125–128].

agreement (of about 3%) is observed between the present radiative lifetimes and the calculated results from Ref. [77] for $v'=0$ and a better agreement (of about 0.5%) is observed for $v'=1$. Whereas our results deviate greatly from the experimental results measured by Rogers and Anderson [153].

5.6. CN transitions

Fig. 7(a) presents the vibrational radiative lifetimes of the $A^2\Pi_i$ electronic state of CN. As shown, the vibrational radiative lifetimes calculated using the ETMF of Ref. [171] are in good agreement with most of the theoretical results [28,82,126], although the radiative lifetimes of da Silva and Dueck [26] calculated utilizing the ETMF of Ref. [155] appear slightly higher than the other calculated results. As shown in Fig. 7(a), large deviations are observed between the calculated values and the experimental results. Besides, the distribution of different experimental radiative lifetimes is so disorderly that the difference between two experimental results for the same vibrational level is up to more than 50% relative to the larger radiative lifetime. Therefore, we assume that the theoretical results are more convincing, just as pointed out by Kuznetsova and Stepanov [154].

Fig. 7(b) illustrates the vibrational radiative lifetimes of the $B^2\Sigma^+$ electronic state of CN. One of them is obtained by experimental measurement and the others are derived from calculations. As shown, our calculated radiative lifetimes are in very good agreement with theoretical results from Refs. [26,28,82,126] except those of Ref. [125]. Compared to the only experimental results measured by Duric et al. [128] we can find in the literature, a good agreement is observed for $v'=2$, 3, 4, 5 and a large discrepancy of about 7% is observed for $v'=0$, 1. Note that the Violet system and the LeBlanc system are both considered to contribute to the radiative lifetimes of CN $B^2\Sigma^+$ electronic state. As for these two electronic transition systems, Knowles et al. [82] and Bauschlichler et al. [155] give two different sets of ETMFs, which both provide a good reproduction of the experimental radiative lifetimes. Here we

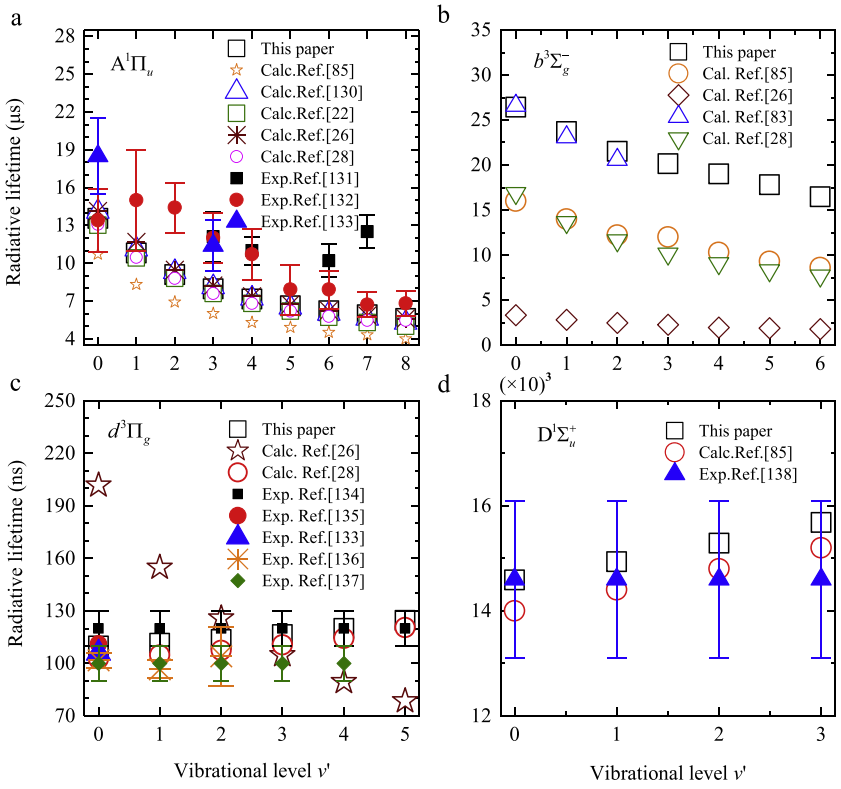

Fig. 8. Comparison of the vibrational radiative lifetimes calculated in the present work for C_2, **(a)** $A^1\Pi_u$ electronic state with the results of Refs. [22,26,28,85,130–133], **(b)** $b^3\Sigma_g^-$ electronic state with the results of Refs. [26,28,83,85], **(c)** $d^3\Pi_g$ electronic state with the results of Refs. [26,28,133–137], **(d)** $D^1\Sigma_u^+$ electronic state with the results of Refs. [85,138].

select the ETMFs of Ref. [82]. It also should be noted that the results in Fig. 7(b) by da Silva and Dudeck exclude the LeBlanc system.

5.7. C_2 transitions

For the Philips, Ballik and Ramsay, Swan and $d^3\Pi_g - c^3\Sigma_u^+$ systems, we select the latest "ab-initio" ETMFs of Ref. [83] because they cover a wider range of internuclear distances than those of other references. In the case of Philips system, it has been widely studied theoretically and experimentally. Fig. 8(a) shows the vibrational radiative lifetimes of the $A^1\Pi_u$ electronic state of C_2. As shown, the present calculated radiative lifetimes are in quite good agreement (of about 4%) with calculations of Refs. [22,26,28,130] except those of Ref. [85]. However, our results are significantly lower than available experimental results of Refs. [131–133], though the radiative lifetimes for $v' = 0$, 1, 5–8 are inside the error bars of Ref. [132]. for the Ballik and Ramsay system. Fig. 8(b) gives some theoretical radiative lifetimes of the $b^3\Sigma_g^-$ electronic state of C_2. A very good agreement (within 4%) between the present radiative lifetimes and the ones calculated by Kokkin et al. [83] is observed for $v' = 0$, 1, 2. Nevertheless, discrepancies of about 36% (or 88%) remain between our calculated results and theoretical results reported in Ref. [28,85] (or Ref. [26]) relative to present radiative lifetimes. As to the two other systems, they both contribute to vibrational radiative lifetimes of $d^3\Pi_g$ electronic state of C_2 and the detailed comparisons between the present radiative lifetimes and various results in the literature are given in Fig. 8(c). Moreover, a large deviation among different experimental results can be seen and our results are in good agreement with the values of Ref. [133–135]. It should also be noticed that our results are in excellent agreement with the calculations of Ref. [28], although they deviate greatly from the calculations of Ref. [26].

Concerning the Mulliken system, the theoretical ETMF of Bruna and Wright [84] is used in this paper. The radiative lifetimes calculated from this ETMF are slightly higher than the experimental results of Ref. [138], but inside the error bars, just as shown in Fig. 8(d). And a slight higher difference (about 5%) can be found in our calculated results compared to the theoretical results from Ref. [85].

For the Deslandres–D'Azambuja system, we use the ETMF of Ref. [85] rather than that of Cooper and Nicholls [156,157], as recommended by Lino da Silva and Dudeck [36], who consider that the results of Ref. [85] are more accurate. However, there is a deviation of 6% between this ETMF and experimental value [85].

As for the Fox–Herzberg system, Chabalowski et al. [85] and Cooper et al. [156] give two ab-initio ETMFs, which are very close. The ETMF of Ref. [85] is chosen in this paper because it covers a wider range of internuclear distances.

5.8. CO^+ transitions

For Comet–Tail, Baldet–Johnson and First-negative systems, we select the ETMFs of Ref. [81], which enable to obtain a good agreement with the available experimental radiative lifetimes, just as shown in Fig. 9. For the $A^2\Pi_i$ electronic state, the calculated radiative lifetimes are in quite good agreement with the theoretical results of Ref. [28] and the experimental results of Refs. [139,140]. For the $B^2\Sigma^+$ electronic state, a very good agreement (of about 1%) between our results and the calculations of Ref. [28] is observed for $v' = 0$–2, whereas the radiative lifetime at $v' = 3$ of Ref. [28] is quite larger than the present result and experimental results of Refs. [141–143]

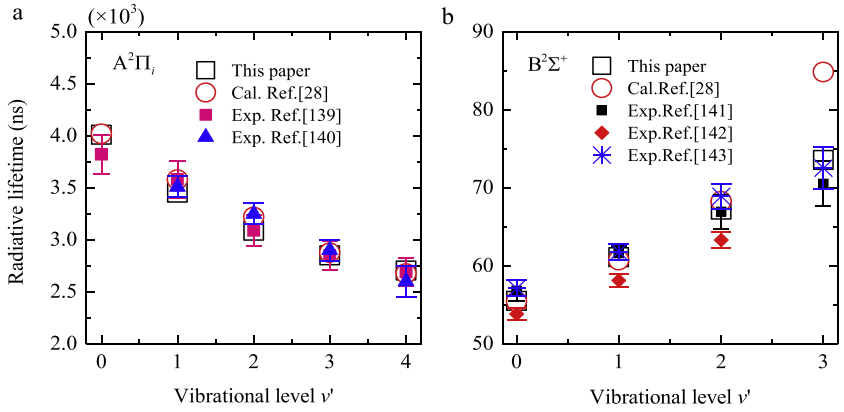

Fig. 9. Comparison of the vibrational radiative lifetimes calculated in the present work for CO^+, **(a)** $A^2\Pi_i$ electronic state with the results of Refs. [28,139–140], **(b)** $B^2\Sigma^+$ electronic state with the results of Refs. [28,139–143].

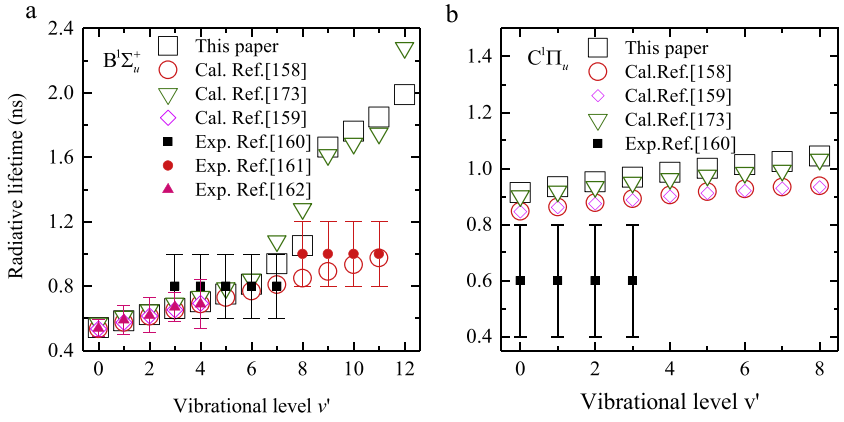

Fig. 10. Comparison of the vibrational radiative lifetimes calculated in the present work for H_2, **(a)** $B^1\Sigma_u^+$ electronic state with the results of Refs. [173,158–162], **(b)** $C^1\Pi_u$ electronic state with the results of Refs. [158–160,173].

5.9. H_2 transitions

For the two electronic transition systems of H_2 considered here, we use the ETMFs given by Drira et al. [86]. Vibrational radiative lifetimes of the $B^1\Sigma_u^+$ and $C^1\Pi_u$ electronic states are calculated with the ETMFs and our vibrational wave functions. Comparisons between our calculated results and experimental data are shown in Fig. 10(a) for the $B^1\Sigma_u^+$ electronic state. A quite good agreement between the calculated radiative lifetimes and the ones measured by Hesser et al. [160] and Schmoranzer et al. [162] is observed, while a large discrepancy of about 33% is observed for $v' = 9$–11. This discrepancy was explained by Fantz et al. [173] who believed that different input spectroscopic constants and ETMFs will lead to large deviations for higher vibrational levels. As shown, the latest theoretical results of Fantz et al. [144,173] are also chosen to validate our calculated results and an excellent agreement is noticed in Fig. 10(a). For the $C^1\Pi_u$ electronic state, our calculated radiative lifetimes agree well with some theoretical results [158,159,173], but a large discrepancy is observed for $v' = 0-3$ compared to the only experimental results [160] we can find in the literature, as shown in Fig. 10(b).

6. Conclusions

In conclusion, we have provided more detailed and accurate tables of the radiative transition probabilities for the main diatomic electronic transition systems contributing to the radiative processes encountered in plasmas produced in Earth, Mars and Jupiter atmospheric entry. The main electronic systems of N_2, N_2^+, NO, O_2, CO, CO^+, CN, C_2 and H_2 have been investigated. The potential energy curves of each electronic state of interest were reconstructed using the RKR inversion procedure based on the most up-to-date spectroscopic constants. Then the radial Schrödinger equation was solved to obtain the vibrational wave functions. These results, together with the latest published "ab-initio" ETMFs were used to calculate some tables of radiative transition probabilities for the main molecular radiative transitions, which are provided in the supplementary material. These arrays can be used to compute the spectral emission and absorption coefficients for the diatomic bound-bound transitions. The radiative lifetimes can also be used to research the collisional-radiative processes in nonequilibrium plasmas.

Acknowledgments

This work was supported by the National Natural Science Foundation of China (No.51421063). ZQ sincerely thanks Robert J. Le Roy's kind guidance of RKR1 codes.

Appendix A. Selected spectroscopic constants

Table A.1
Klein–Dunham coefficients for the selected states of the N_2 molecule (all values are in cm^{-1} except r_e in Angstrom and v_{max}).

	Y_{ij}	0	1	2	3	4	5	6	E_{diss}	r_e	v_{max}
$X^3\Sigma_g^+$ [37,163]	0	0.0	2358.56	14.317	−3.31E−3	−1.95E−4			79886.6	1.097685	15
	1	1.998236	1.730986E−2	−3.01203E−5	−6.927E−8						
	2	5.73729E−6	8.951E−9								
$A^3\Sigma_u^+$ [38,163]	0	50203.6	1460.94	13.98	2.4E−2	−2.56E−3			30135.8	1.2866	16
	1	1.4539	1.75E−2	−1.4E−4							
	2	5.46E−6	1.1E−7								
$B^3\Pi_g$ [38,163]	0	59619.3	1734.025	14.412	−3.3E−3	−7.9E−4	4.2E−5	−1.68E−6	39811.7	1.2126	21
	1	1.63772	1.793E−2	−1.0E−4	5.0E−6	−2.1E−7					
	2	5.88E−6	1.3E−8								
$W^3\Delta_u$ [39,163]	0	59808	1506.5	12.5					39301	1.2784	17
	1	1.47	1.71E−2								
$B'^3\Sigma_u$ [40,163]	0	66272.4	1516.6	12					42452	1.2784	21
	1	1.473	1.666E−2								
	2	5.55E−6									
$C^3\Pi_u$ [41,163]	0	89136.9	2047.79	28.942	2.25	−0.551			10140.7	1.14869	4
	1	1.8268	2.4E−2	1.9E−3	−6.0E−4						
	2	5.1E−6	2.2E−6	−1.3E−6	2.4E−7						
$a^1\Pi_g$ [40,163]	0	69283.1	1694.2	13.949					49051	1.2203	10
	1	1.6169	1.793E−2								
	2	5.89E−5									

Table A.2
Klein–Dunham coefficients for the selected states of the N_2^+ molecule (all values are in cm^{-1} except r_e in Angstrom and v_{max}).

	Y_{ij}	0	1	2	3	4	5	6	7	E_{diss}	r_e	v_{max}
$X^2\Sigma_g^+$ [36,164]	0	0.0	2197.95	16.0906	4.0E−3	−6.1E−3	3.9E−4	1.4E−5	2.0E−7	71368	1.1191	21
	1	1.92286	1.8634E−2	−6.77E−5	−2.32E−6							
	2	5.92E−6	3.9E−8									
$A^2\Pi_u$ [36,164]	0	9167.46	1900.73	14.9618	1.12E−2	−0.27E−3				62352	1.1772	27
	1	1.73539	1.8652E−2	−6.0E−5	−1.1E−6							
	2	5.6E−6										
$B^2\Sigma_u^+$ [36,164]	0	25461.11	2406.67	23.3782	−0.3	−6.67E−2				45799	1.0771	4
	1	2.07492	2.088	−5.0E−4	−8.8E−5							
	2	6.17E−6										
$C^2\Sigma_u^+$ [36,165]	0	64609.05	2069.4	−8.3	1.6E−2					26057.15	1.2628	6
	1	1.5098	−1.0E−3									

Table A.3
Klein–Dunham coefficients for the selected states of the NO molecule (all values are in cm^{-1} except r_e in Angstrom and v_{max}).

	Y_{ij}	0	1	2	3	4	5	6	7	E_{diss}	r_e	v_{max}
$X^2\Pi_r$ [42]	0	0.0	1904.13	14.08836	1.00467E−2	−1.5331E−4	−9.769E−6	−1.9142E−7	5.2734E−9	53344	1.15077	22
	1	1.704888	0.01754158	1.4886E−5		−4.7275E−8	1.0108E−9	−6.0557E−11				
	2	5.466E−6	1.7032E−8									
$A^2\Sigma^+$ [40]	0	43965.7	2374.31	16.106	4.65E−2					28603	1.0634	8
	1	1.9965	1.915									
	2	5.4E−6										
$B^2\Pi_r$ [43]	0	45932.3	1042.4	7.7726	0.11596	−3.9577e−3				26637	1.4167	28
	1	1.1244	0.013433	2.991Ee−5	3.177E−6							
	2	5.2E−6	1.4E−8									
$C^2\Pi_r$ [43]	0	52179.8	2381.3	15.702	7.253E−2					20383	1.062	9
	1	2.0155	3.244E−2									
	2	5.8E−6	1.8E−8									
$D^2\Sigma^+$ [40]	0	53084.7	2323.9	22.885	0.75	−0.22				19484	1.0618	5
	1	2.0026	2.175									
	2	5.9E−6	5.9E−8									
$B'^2\Delta$ [44]	0	60364.2	1217.4	15.61						12205	1.302	6
	1	1.332	2.1E−2									
$E^2\Sigma^+$ [40]	0	60628.8	2375.3	16.43						11940	1.06615	4
	1	1.9863	1.82E−2									
	2	5.6E−6										

Table A.4
Klein–Dunham coefficients for the selected states of the O_2 molecule (all values are in cm^{-1} except r_e in Angstrom and v_{max}).

	Y_{ij}	0	1	2	3	4	5	6	7	E_{diss}	r_e	v_{max}
$X^3\Sigma_g^-$	0	0.0	1580.1932	11.980804	0.047474736	−1.72748E−3				42048	1.20752	19
[23,163]	1	1.445622	0.01593268	6.406456E−5	−2.846158E−6							
	2	4.839E−6	2.06E−6									
$B^3\Sigma_u^-$	0	49793.3	709.0577	10.61408	−0.059212435	−0.023974994	2.2067951E−3	−1.5990957E−4	4.4274814E−6	8556.5	1.60426	21
[35,163]	1	0.818975	0.0119225	−6.30472E−4	1.57426E−6	6.70586E−6	−9.35318E−7	2.901E−8				
	2	4.55E−6	2.2E−7									

Table A.5
Klein–Dunham coefficients for the selected states of the CO molecule (all values are in cm^{-1} except r_e in Angstrom and v_{max}).

	Y_{ij}	0	1	2	3	4	5	6	7	8	9	E_{diss}	r_e	v_{max}
$X^1\Sigma^+$	0	0.0	2169.81267	13.2878763	1.04111E−2	6.93664E−5	1.67935E−7	2.05925E−9	−8.488E−10	1.2388E−11	−8.234E−14	90575.3	1.1327	41
[45,166]	1	1.93128098	1.75044E−2	7.17392E−7	−2.1464E−8	4.4354E−-9	−1.361E−10	1.2458E−12	−2.125E−14					
	2	6.12162E−6	−1.0349E−9	1.8498E−10	−2.431E−12									
$a^3\Pi_r$	0	48686.8	1743.41	14.36	−4.5E−2	2.5E−5						41888.6	1.2105	12
[46,76]	1	1.69124	1.904	−4.1E−5										
	2	6.36E−6	4.0E−8											
$a'^3\Sigma^+$	0	55825.5	1228.6	10.466	9.1Ee−3	2.59E−3						34842.9	1.3523	9
[40]	1	1.3446	1.892E−2											
	2	6.41E−6												
$d^3\Delta_i$	0	61120.1	1171.94	10.635	7.85E−2	−1.63E−5						29519	1.3740	10
[40,76]	1	1.3108	1.782E−2	1.13E−4										
	2	6.59E−6												
$A^1\Pi$	0	65075.8	1518.24	19.4	0.76584	−0.14117	0.01434	−8.051E−4	2.36E−5	2.9E−7		25499.6	1.2408	19
[47,168]	1	1.6115	0.023251	1.5911E−3	−5.716E−4	8.2417E−5	−5.9413E−6	2.1149E−7	2.991E−9					
	2	7.29E−6	1.05E−7											
$B^1\Sigma^+$	0	86932.16	2150.41	34.09								3643.14	1.1197	2
[48]	1	1.96103	2.574E−2											
	2	6.477E−6	5.86E−7											
$b^3\Sigma^+$	0	83686.5	2333.9	58.64								5908.5	1.113	2
[49]	1	1.986	4.2E−2											

Table A.6
Klein–Dunham coefficients for the selected states of the CO^+ molecule (all values are in cm^{-1} except r_e in Angstrom and v_{max}).

	Y_{ij}	0	1	2	3	E_{diss}	r_e	v_{max}
$X^2\Sigma^+$ [56,167]	0	0.0	2214.127	15.094	−1.17E−2	68288.8	1.11514	5
	1	1.976941	1.8943E−2	−3.44E−6				
	2	6.313E−6	1.53E−8					
$A^2\Pi_i$ [56,167]	0	207332.037	1561.806	13.4785	8.65Ee−3	47556.8	1.24377	8
	1	1.589392	1.9494E−2	−1.17E−7				
	2	6.729E−6	−3.84E−8					
$B^2\Sigma^+$ [57,81]	0	45876.7	1734.57	28.248	0.399	38279.6	1.16877	2
	1	1.7999	3.025E−2					
	2	7.75E−6	2.2E−7					

Table A.7
Klein–Dunham coefficients for the selected states of the CN molecule (all values are in cm^{-1} except r_e in Angstrom and v_{max}).

	Y_{ij}	0	1	2	3	4	5	6	7	E_{diss}	r_e	v_{max}
$X^2\Sigma^+$	0	0.0	2068.6834	13.12172	−5.412E−2	−9.83E−5	3.23E−5			63296.6	1.1718073	11
[54,169]	1	1.8997835	0.01737487	−2.43E−5	−4.92E−7	−1.61E−8						
	2	6.41E−6	1.2E−8									
$A^2\Pi_i$	0	9240	1813.26	12.76873	−3.569E−3	1.070745E−4	−4.6648E−6	−2.5273E−7		54053.3	1.2333	20
[59]	1	1.71591	1.716732E−2	−5.4905E−5	6.759374E−6	5.88513E−7	1.890441E−8	−2.34754E−10				
	2	5.93E−6	4.2E−8									
$B^2\Sigma^+$	0	25752	2161.46	18.219	−0.486	0.04	−6.93E−3	4.32E−4	−8.34E−6	56777	1.150	17
[60,169]	1	1.96891	2.0337E−2	−5.9E−5	−7.71E−5	3.1E−6						
	2	6.5322E−6	8.0725E−8									

Table A.8
Klein–Dunham coefficients for the selected states of the C_2 molecule (all values are in cm^{-1} except r_e in Angstrom and v_{max}).

	Y_{ij}	0	1	2	3	4	5	E_{diss}	r_e	v_{max}
$X^1\Sigma_g^+$ [50,170]	0	0.0	1855.01	13.555	−0.132	3.57E−3	−1.116E−3	50247.9	1.2425	6
	1	1.8201	1.801E−2	−6.33E−5	−2.06E−6					
	2	6.964E−6	6.41E−8							
$a^3\Pi_u$ [51,163]	0	716.2	1641.35	11.670				49531.7	1.3119	9
	1	1.6342	1.661							
	2	6.44E−6								
$b^3\Sigma_g^-$ [52,163]	0	6434.8	1470.4	11.155	1.39E−2			43812	1.36928	6
	1	1.4986	1.631E−2	−4.61E−6						
	2	6.1958E−6	6.62E−9							
$A^1\Pi_u$ [53,170]	0	8391.3	1608.2	12.055	−0.012			41867	1.3184	8
	1	1.6165	1.687E−2	−5.47E−5						
	2	6.494E−6	3E−8							
$c^3\Sigma_u^+$ [40,163]	0	9124.2	2085.9	18.623				37988.4	1.23	9
	1	1.921	1.255E−2							
$d^3\Pi_g$ [54,163]	0	20022.5	1788.22	16.457	−0.501			30225.4	1.2661	10
	1	1.75523	1.907E−2	5.35E−4						
	2	6.74E−6								
$e^3\Pi_g$ [55,163]	0	40796.7	1106.56	39.26	2.81	−0.127		19643.9	1.5351	4
	1	1.1922	2.42E−2							
	2	6.3E−6								
$D^1\Sigma_g^+$ [40,163]	0	43239.8	1829.57	13.94				39843.5	1.2380	3
	1	1.8332	1.96E−2							
	2	7.32E−6								

Table A.9
Klein–Dunham coefficients for the selected states of the H_2 molecule (all values are in cm^{-1} except r_e in Angstrom and v_{max}).

	Y_{ij}	0	1	2	3	4	5	6	7	8	E_{diss}	r_e	v_{max}
$X^1\sum_g^+$ [61]	0	0.0	4432.29142	−149.2039	12.01408	−2.369503	0.2852839	−0.020446	7.82E−04	−1.27E−05	38163.37	0.74152	14
	1	61.264895	−4.274626	1.0029705	−0.329079	0.057094	−5.38E−03	2.59E−04	−5.04E−06				
	2	−0.049649	0.0106961	−6.00E−03	1.64E−03	−2.18E−04	1.38E−05	−3.35E−07					
	3	5.80E−05	−2.84E−05	1.46E−05	−3.05E−06	2.73E−07	−8.75E−09						
	4	−7.00E−08	4.25E−08	−1.69E−08	2.39E−09	−1.08E−10							
	5	6.39E−11	−3.54E−11	9.45E−12	−6.70E−13								
	6	−3.81E−14	1.54E−14	−2.06E−15									
$B^1\sum_u^+$ [62]	0	91528.4	1357.19	−20.15	0.46	−0.021					28767.93	1.2894	6
	1	19.984	−1.115	0.0836	−0.0044								
	2	−0.01656	2.08E−3	−0.00013									
$C^1\prod_u$ [62]	0	100089.8	2443.77	−69.524	0.7312	−0.0415					20236.8	1.03346	13
	1	31.3629	−1.6647	0.0296	−0.00296								
	2	−0.0223	0.00074										

Appendix B. Supplementary material (in .CSV) files

Supplementary material associated with this article can be found, in the online version, at doi:10.1016/j.jqsrt.2017.08.010. The tables of supplementary material give the Einstein coefficients in s^{-1}, absorption band oscillator strengths and Franck–Condon factors corresponding to the upper v' vibrational levels in columns and the lower v'' vibrational levels in rows.

References

[1] Laux CO, Spence TG, Kruger CH, Zare RN. Optical diagnostics of atmospheric pressure air plasmas. Plasma Sources Sci Technol 2003;12(2):125–38.
[2] Hanson RK, Spearrin RM, Goldenstein CS. Spectroscopy and optical diagnostics for gases. New York: Springer; 2015.
[3] Kurucz RL. Recent directions in astrophysical quantitative spectroscopy and radiation hydrodynamics. AIP Conf Proc 2009:1171.
[4] Ung AYM. Emission from the afterglow of an ozonizer discharge through nitrogen. Chem Phys Lett 1975;32(1):193–6.
[5] Golde MF, Thrush BA. Afterglows. Rev Prog Phys 2001;36(10):1285–364.
[6] Park C. Nonequilibrium hypersonic aerothermodynamics. New York: Wiley; 1990.
[7] Perrin MY, Colonna G, D'Ammando G, Pietanza LD, Ph Riviere, Soufani A, Surzhikov S. Radiation models and radiation transfer in hypersonics. Open Plasma Phys J 2014;7(1):114–26.
[8] Annaloro J, Bultel A. Vibrational and electronic collisional-radiative model in air for Earth entry problems. Phys Plasmas 2014;21(12):251–61.
[9] Nicholls RW, Stewart AL. Allowed transitions. New York: Academic Press; 1962.
[10] Nicholls RW. On the electronic transition moment variation and the r–centroid approximation in interpretation of spectral intensities of diatomic molecules. J Quant Spectrosc Radiat Transf 1974;14(14):233–7.
[11] Cramer CJ. Essentials of computational chemistry: theories and models. New York: John Wiley & Sons; 2004.
[12] Rydberg R. Graphische darstellung einiger bandenspektroskopischer ergebnisse. Z Phys 1932;73(5-6):376–85.
[13] Klein O. Zur berechnung von potentialkurven für zweiatomige moleküle mit hilfe von spektraltermen. Z Phys 1932;76(3):226–35.
[14] Rees ALG. The calculation of potential-energy curves from band-spectroscopic data. Proc Phys Soc 1947;59(6):998.
[15] Gilmore FR, Laher RR, Espy PJ. Franck-condon factors, r-centroids, electronic transition moments, and Einstein coefficients for many nitrogen and oxygen band systems. J Phys Chem Ref Data 1992;21(5):1005–107.
[16] Krupenie PH. The spectrum of molecular oxygen. J Phys Chem Ref Data 1972;1(2):423–534.
[17] Lofthus A, Krupenie PH. The spectrum of molecular nitrogen. J Phys Chem Ref Data 1977;6(1):113–307.
[18] Saxon RP, Slanger TG. Molecular oxygen absorption continua at 195-300 nm and O_2 radiative lifetimes. J Geophys Res 1986;91:9877–9.
[19] Marinelli WJ, Green BD, Defaccio MA, Blumberg WAM. Vibrational relaxation and intersystem crossing in N_2 $a^1\Pi_g$. J Phys Chem 1988;92(12):3429–37.
[20] Piper LG, Cowles LM. Einstein coefficients and transition moment variation for the NO ($A^2\Sigma^+ - X^2\Pi$) transition. J Chem Phys 1986;85(2):88–94.
[21] Costes M, Naulin C, Dorthe G. Einstein coefficient of the CN $B^2\Sigma^+ - A^2\Pi_i$ (0,0) band. Chem Phys Lett 1985;113(6):569–72.
[22] Langhoff SR, Bauschlicher CW, Rendell AP, Komornicki A. Theoretical study of the radiative lifetime of the $A^1\Pi_u$ state of C_2. J Chem Phys 1990;92(11):6599–603.
[23] Laux CO, Kruger CH. Arrays of radiative transition probabilities for the N_2 first and second positive, NO beta and gamma, N_2^+ first negative and O_2 Schumann–Runge band systems. J Quant Spectrosc Radiat Transf 1992;48(1):9–24.

[24] Peyrou B, Chemartin L, Lalande P, Chéron BG, Rivière P, Perrin MY, Soufiani A. Radiative properties and radiative transfer in high pressure thermal air plasmas. J Phys D: Appl Phys 2012;45(45):455203.

[25] Jain DC. Einstein A coefficients, band oscillator strengths and absolute band strengths for the Comet–Tail band system of CO^+. J Phys B Atom Molec Phys 1973;5(2):199–203.

[26] Lino da Silva M, Dudeck M. Arrays of radiative transition probabilities for CO_2–N_2 plasmas. J Quant Spectrosc Radiat Transf 2006;102(3):348–86.

[27] Chauveau S, Perrin MY, Rivière P, Soufiani A. Contributions of diatomic molecular electronic systems to heated air radiation. J Quant Spectrosc Radiat Transf 2002;72(4):503–30.

[28] Babou Y, Rivière P, Perrin MY, Soufiani A. Spectroscopic data for the prediction of radiative transfer in CO_2-N_2 plasmas. J Quant Spectrosc Radiat Transf 2009;110(1-2):89–108.

[29] Roy RJL. RKR1: a computer program implementing the first-order RKR method for determining diatomic molecule potential energy functions. J Quant Spectrosc Radiat Transf 2016;186:158–66.

[30] Maitland GC. Intermolecular forces: their origin and determination. England: Oxford University Press; 1981.

[31] Zare RN. Calculation of intensity distribution in the vibrational structure of electronic transitions: the $B^3\Pi_{0^+u} - X^1\Sigma_{0^+g}$ resonance series of molecular iodine. Chem Phys 1964;40(7):1934–44.

[32] Hulburt HM, Hirschfelder JO. Potential energy functions for diatomic molecules. J Chem Phys 1941;9(9):61–9.

[33] Schadee A. Unique definitions for the band strength and the electronic-vibrational dipole moment of diatomic molecular radiative transitions. J Quant Spectrosc Radiat Transf 1978;19(4):451–3.

[34] Roy RJLLEVEL. A computer program for solving the radial Schrödinger equation for bound and quasibound levels. J Quant Spectrosc Radiat Transf 2016;186:167–78.

[35] Cheung SC, Yoshino K, Parkinson W, Freeman D. Molecular spectroscopic constants of O_2 ($B^3\Sigma_u^-$): the upper state of the Schumann–Runge bands. J Mol Spectrosc 1986;119(1):1–10.

[36] Klynning L, Pages P. The band spectrum of N_2^+. Phys Scr 1982;25(4):543.

[37] Edwards S, Roncin JY, Launay F, Rostas F. The electronic ground state of molecular nitrogen. J Mol Spectrosc 1993;162(1):257–67.

[38] Roux F, Michaud F, Vervloet M. High-resolution Fourier spectrometry of $^{14}N_2$: analysis of the (0–0), (0–1), (0–2), (0–3) bands of the $C^3\Pi_u - B^3\Pi_g$ system. Can J Phys 1989;67(2-3):143–7.

[39] Werner H, Kalcher J, Reinsch E. Accurate ab-initio calculations of radiative transition probabilities between the $A^3\Sigma_u^+$, $B^3\Pi_g$, $W^3\Delta_u$, $B'^3\Sigma_u^-$, and $C^3\Pi_u$ states of N_2. J Chem Phys 1984;81(81):2420–31.

[40] Huber KP, Herzberg G. Molecular spectra and molecular structure 4: constants of diatomic molecules. New York: Springer; 1979.

[41] Roux F, Michaud F, Vervloet M. High-resolution Fourier spectrometry of $^{14}N_2$ violet emission spectrum: extensive analysis of the $C^3\Pi_u - B^3\Pi_g$ system. J Mol Spectrosc 1993;158(2):270–7.

[42] Amiot C. The infrared emission spectrum of NO: Analysis of the Δv=3 sequence up to v=22. J Mol Spectrosc 1982;94(1):150–72.

[43] Gallusser R, Dressler K. Multistate vibronic coupling between the excited $^2\Pi$ states of the NO molecule. J Chem Phys 1982;76(9):4311–27.

[44] Jungen C. Vacuum-ultraviolet emission and absorption spectrum of the NO molecule: the $^2\Delta$ states and their interactions. Can J Phys 1966;44(12):3197–216.

[45] Farrenq R, Guelachvili G, Sauval AJ, Grevesse N, Farmer CB. Improved Dunham coefficients for CO from infrared solar lines of high rotational excitation. J Mol Spectrosc 1991;149(2):375–90.

[46] Field RW, Tilford SG, Howard RA, Simmons JD. Fine structure and perturbation analysis of the $a^3\Pi$ state of CO. J Mol Spectrosc 1972;44(2):347–82.

[47] Simmons JD, Bass AM, Tilford SG. The Fourth positive system of carbon monoxide observed in absorption at high resolution in the vacuum ultraviolet region. Astrophys J 1969;155:345–58.

[48] Eidelsberg M, Roncin JY, Floch AL, Launay F, Letzelter C, Rostas J. Reinvestigation of the vacuum ultraviolet spectrum of CO and isotopic species: The $B^1\Sigma^+ - X^1\Sigma^+$ transition. J Mol Spectrosc 1987;121(2):309–36.

[49] Prasad CVV, Bhale GL, Reddy SP. The Third positive ($b^3\Sigma^+ - a^3\Pi_r$) system of CO: observation of the $v=2$ level of $b^3\Sigma^+$☆. J Mol Spectrosc 1987;121(2):261–9.

[50] Douay M, Nietmann R, Bernath PF. New observations of the $A^1\Pi_u - X^1\Sigma_g^+$ transition (Phillips system) of C_2. J Mol Spectrosc 1988;131(2):250–60.

[51] Phillips JG, Davis SP. The Swan system of the C2 molecule: the spectrum of the HgH molecule. 1968, USA: University of California Press;1968.

[52] Amiot C, Chauville J, Maillard JP. New analysis of the C_2 Ballik–Ramsay system from flame emission spectra. J Mol Spectrosc 1979;75(1):19–40.

[53] Marenin IR, Johnson HR. New molecular constants for the Phillips system of C_2☆. J Quant Spectrosc Radiat Transf 1970;10(4):305–9.

[54] Prasad CVV, Bernath PF. Fourier transform spectroscopy of the Swan ($d^3\Pi_g - a^3\Pi_u$) system of the jet-cooled C_2 molecule. Astrophys J 1994;426(2):812–21.

[55] Phillips JG. The Fox–Herzberg system of the C_2 molecule. Astrophys J 1949;110(1):73.

[56] Kępa R, Kocan A, Ostrowska-Kopeć M, Piotrowska-Domagala I, Zachwieja M. New spectroscopic studies of the Comet–Tail ($A^2\Pi_i - X^2\Sigma^+$) system of the CO^+ molecule. J Mol Spectrosc 2004;228(1):66–75.

[57] Bembenek Z, Domin U, Kepa R, Porada K, Rytel M, Zachwieja M, Jakubek Z, Janjic JD. New bands and new analyses in the spectrum of the Baldet–Johnson ($B^2\Sigma^+ - A^2\Pi_i$) system of CO^+. J Mol Spectrosc 1994;165(1):205–18.

[58] Capitelli M, Colonna G, D'Ammando G, Hassouni K, Laricchiuta A, Pietanza LD. Coupling of plasma chemistry, vibrational kinetics, collisional-radiative models and electron energy distribution function under non-equilibrium conditions. Plasma Process Polym 2017;14(1-2):1–11.

[59] Ito H, Kazama A, Kuchitsu K. Perturbations in the CN ($B^2\Sigma^+ - X^2\Sigma^+$) tail band system Part 4. The $B^2\Sigma^+ - A^2\Pi_i$ perturbations in the v_B= 11, 14–16, 18 and 19 levels. J Mol Struct 1994;324(1–2):29–43.

[60] Ito H, Ozaki Y, Suzuki K, Kondow T, Kuchitsu K. Analysis of the $B^2\Sigma^+ - A^2\Pi_i$ perturbations in the CN ($B^2\Sigma^+ - X^2\Sigma^+$) main band system: Electronic structures of $B^2\Sigma^+$ and $A^2\Pi_i$. J Mol Spectrosc 1988;127(1):143–55.

[61] Irwin AW. Refined diatomic partition functions. I. Calculational methods and H_2 and CO results. Astron Astrophys 1987;182:348–58.

[62] Dabrowski I. The Lyman and Werner bands of H2.. Can J Phys 1984;62(12):1639–64.

[63] Werner H, Kalcher J, Reinsch E. Accurate ab-initio calculations of radiative transition probabilities between the $A^3\Sigma_u^+$, $B^3\Pi_g$, $W^3\Delta_u$, $B'^3\Sigma_u^-$, and $C^3\Pi_u$ states of N_2. J Chem Phys 1984;81(81):2420–31.

[64] Allison AC, Guberman SL, Dalgarno A. A model of the Schumann–Runge continuum of O_2. J Geophys Res 1986;91(A9):10193–8.

[65] Friedman RS. Oscillator strengths of the Schumann–Runge bands of isotopic oxygen molecules. J Quant Spectrosc Radiat Transf 1990;43(3):225–38.

[66] Langhoff SR, Jr CWB, Partridge H. Theoretical study of the N_2^+ Meinel system. J Chem Phys 1987;87(8):4716–21.

[67] Langhoff SR, Jr CWB. Theoretical study of the first and second negative systems of N_2^+. J Chem Phys 1988;88(1):329–36.

[68] Settersten TB, Patterson BD, Iv WHH. Radiative lifetimes of NO $A^2\Sigma^+$ (v′=0,1,2) and the electronic transition moment of the $A^2\Sigma^+ - X^2\Pi$ system. J Chem Phys 2009;131(10):7405.

[69] Langhoff SR, Partridge H, Jr CWB, Komornicki A. Theoretical study of the NO β system. J Chem Phys 1991;94(8):6638–43.

[70] Cooper DM. Theoretical study of IR band intensities and electronic transition moments for the β and δ systems of NO. J Quant Spectrosc Radiat Transf 1982;27(4):459–65.

[71] Sheehy JA, Jr CWB, Langhoff SR, Partridge H. Theoretical study of the nitric oxide ϵ and 11000Å bands. Chem Phys Lett 1994;225(1–3):221–8.

[72] Vivie RD, Peyerimhoff SD. Theoretical spectroscopy of the NO radical. I. Potential curves and lifetimes of excited states. J Chem Phys 1988;89(5):3028–43.

[73] Rawlins WT, Person JC, Fraser M E, Miller SM, Blumberg WAM. The dipole moment and infrared transition strengths of nitric oxide. J Chem Phys 1998;109(9):3409–17.

[74] Langhoff SR, Jr CWB. Global dipole moment function for the $X^1\Sigma^+$ ground state of CO. J Chem Phys 1994;102(13):5220–5.

[75] Spielfiedel A, Tchang-Brillet W-ÜL, Dayou F. Feautrier. Ab initio calculation of the dipole transition moment and band oscillator strengths of the CO (A-X) transition. Astron Astrophys 1999;346(2):699–704.

[76] Lu PF, Yan L, Yu ZY, Gao YF, Gao T. An accurate calculation of potential energy curves and transition dipole moment for low-lying electronic states of CO. Commun Theor Phys 2013;59(2):193–8.

[77] Kirby K, Cooper DL. Theoretical study of low-lying $^1\Sigma^+$ and $^1\Pi$ states of CO. II. Transition dipole moments, oscillator strengths, and radiative lifetimes. J Chem Phys 1989;90(9):4895–902.

[78] Carlson TA, Đurić N, Erman P. Larsson. Correlation between perturbation and collisional transfers in the A, B, C, and b states of CO as revealed by high resolution lifetime measurements. Z Phys A 1978;287(2):123–36.

[79] Slanger TG, Black G. Relative electronic transition moments for the triplet system ($d^3\Delta - a^3\Pi$) of CO. J Phys B Atom Mol Phys 1972;5:1988–92.

[80] Peterson KA, Woods RC. Theoretical dipole moment functions involving the $a^3\Pi$ and $a'^3\Sigma^+$ states of carbon monoxide. J Chem Phys 1990;93(7):5029–36.

[81] Okada K, Iwata S. Accurate potential energy and transition dipole moment curves for several electronic states of CO^+. J Chem Phys 2000;112(112):1804–8.

[82] Knowles PJ, Werner HJ, Hay PJ, Cartwright DC. The $A^2\Pi_i - X^2\Sigma^+$ red and $B^2\Sigma^+ - X^2\Sigma^+$ violet systems of the CN radical: accurate multireference configuration interaction calculations of the radiative transition probabilities. J Chem Phys 1988;89(89):7334–43.

[83] Kokkin DL, Bacskay GB, Schmidt TW. Oscillator strengths and radiative lifetimes for C_2 Swan, Ballik-Ramsay, Phillips and $d^3\Pi_g - c^3\Sigma_u^+$ systems. J Chem Phys 2007;126(8):084302.

[84] Bruna PJ, Wright JS. Theoretical study of the transition probabilities of the doubly-excited states $E^1\Sigma_g^+$ of C_2 and $2^2\Sigma_g^+$ of C_2^+. J Phys Chem 1992;96(4):1630–40.

[85] Chabalowski CF, Peyerimhoff SD, Buenker RJ. The Ballik-Ramsay, Mulliken, Deslandres-d'Azambuja and Phillips systems in C_2: a theoretical study of their electronic transition moments. Chem Phys 1983;81(1–2):57–72.

[86] Drira Il. Ab initio calculation of the electronic transition moments for excited states of the H2 Molecule. 1999; 198(1):52–56.

[87] Shemansky DE. N_2 Vegard–Kaplan system in absorption. J Chem Phys 1969;51(2):689–700.

[88] Shemansky DE, Carleton NP. Lifetime of the N_2 Vegard–Kaplan system. J Chem Phys 1969;51(2):682–8.

[89] Brzozowski J, Erman P, Lyyra M. Predissociation rates and perturbations of the A, B, B', C, D and F states in NO studied using time resolved spectroscopy. Phys Scr 1976;14(6):290.

[90] Smith AJ, Read FH. Measured lifetimes of the $A^2\Sigma^+$, $D^2\Sigma^+$ and $C^2\Pi$ states of NO. J Phys B Atom Mol Phys 1978;11(18):3263.

[91] Piper LG, Holtzclaw KW, Green BD, Blumberg WAM. Experimental determination of the Einstein coefficients for the N_2 (B–A) transition. J Chem Phys 1989;90(10):5337–45.

[92] Shemansky DE. $A^3\Sigma_u^+$ molecules in the N_2 afterglow. J Chem Phys 1976;64(2):565–80.

[93] Eyler EE, Pipkin FM. Lifetime measurements of the $B^3\Pi_g$ state of N_2 using laser excitation. J Chem Phys 1983;79(8):3654–9.

[94] Jeunehomme M. Transition moment of the First positive band system of nitrogen. J Chem Phys 1966;45(5):1805–11.

[95] Carlson T A, Duric N, Erman P, Larsson M. Collisional transfer to the B State in N_2. Phys Scr 1979;19(19):25.

[96] Hollstein M, Lorents DC, Peterson JR, Sheridan JR. Time of flight measurement of N_2 and N_2^+ lifetimes. Can J Chem 1969;47(10):1858–61.

[97] Osherovich AL, Gorshkov VN. Measurement of the radiation lifetimes of the $C^3\Pi_u$ excited state of the N_2 molecule and the $B^2\Sigma_u^-$ excited state of the N_2^+ molecule by the phase-shift and delayed-coincidences methods. Opt Spectrosc 1976;41(1):92–3.

[98] Becker KH, Engels H, Tatarczyk T. Lifetime measurements of the $C^3\Pi_u$ state of nitrogen by laser-induced fluorescence. Chem Phys Lett 1977;51(1):111–15.

[99] Dumont MN, Remy F. The radiative lifetime of the $C^3\Pi_u$ state of N_2. J Chem Phys 1982;76(2):1175–6.

[100] Larsson M, Radozycki T. Time resolved studies of perturbations in the $v'=1$ level and radiative properties of the $C^3\Pi_u$ state in N_2. Phys Scr 1982;25:627–30.

[101] Dahl F, Oddershede J. Radiative lifetime of the forbidden $a^1\Pi_g - X^1\Sigma_g^+$ transition of N_2. Phys Scr 1986;33:135–40.

[102] Marinelli WJ, Kessler WJ, Green BD, Blumberg WAM. The radiative lifetime of N_2 ($a^1\Pi_g$ v = 0-2). Chem Phys 1989;91(91):701–7.

[103] Covey R, Saum KA, Benesch W. Transition probabilities for the $W^3\Delta_u - B^3\Pi_g$ system of molecular nitrogen. J Opt Soc Am 1973;63(5):592–6.

[104] Holland RF, Maier WB. Study of the A–X transitions in N_2^+ and CO^+. J Chem Phys 1972;56(11):5229–46.

[105] Maier W B, Holland R F. A study of visible and near-UV radiation from long-lived states of N_2^+. Bull Am Phys Soc 1972;17(5):695–6.

[106] Peterson JamesR, Moseley JohnT. Time-of-flight determination of lifetimes of N_2^+ ($A^2\Pi_u$) the Meinel band system. J Chem Phys 1973;58(1):172–7.

[107] Johnson AW, Fowler RG. Measured lifetimes of rotational and vibrational levels of electronic states of N_2. J Chem Phys 1970;53(53):65–72.

[108] Fournier P, Runstraat CAVD, Govers T R, Schopman J, Heer FJD, Los J. Collision-induced dissociation of 10 keV N_2^+ ions: evidence for predissociation of the $C^2\Sigma_u^+$ state. Chem Phys Lett 1971;9(5):426–8.

[109] Brzozowski J, Elander N, Erman P. Direct measurements of lifetimes of low–lying excited electronic states in nitric oxide. Phys Scr 1974;9(2):99.

[110] Zacharias H, Halpern JB, Welge KH. Two-photon excitation of NO ($A^2\Sigma^+$ $v'=$ 0, 1, 2) and radiation lifetime and quenching measurements. Chem Phys Lett 1976;43(1):41–4.

[111] Imajo T, Shibuya K, Obi K, Tanaka I. Energy transfer and electronic quenching of the low-lying Rydberg states of nitric oxide in nitric oxide/nitrogen mixtures. J. Phys. Chem 1986;90(22):6006–11.

[112] Tsukiyama K, Munakata T, Tsukakoshi M, Kasuya T. Fluorescence lifetimes of NO $A^2\Sigma^+$ ($v'=$ 3 and 4), $C^2\Pi$ ($v'=$ 0) and $D^2\Sigma^+$ ($v'=$ 0) studied by tunable VUV laser excitation. Chem Phys 1988;121(1):55–62.

[113] Luque J, Crosley DR. Transition probabilities and electronic transition moments of the $A^2\Sigma^+ - X^2\Pi$ and $D^2\Sigma^+ - X^2\Pi$ systems of nitric oxide. J Chem Phys 1999;111(16):7405–15.

[114] Jeunehomme M, Duncan ABF. Lifetime measurements of some excited states of nitrogen, nitric oxide, and formaldehyde. J Chem Phys 1964;41(6):1692–9.

[115] Gadd GE, Slanger TG. NO ($B^2\Pi$) radiative lifetimes: v= 0–6. J Chem Phys 1990;92(4):2194–202.

[116] Gadd GE, Huestis DL, Slanger TG. Rotational-level-dependent radiative lifetimes and branching ratios in NO ($B^2\Pi$) (v= 7, Ω= 1/2, 3/2). J Chem Phys 1991;95(6):3944–54.

[117] D'azy O B, López-Delgado R, Tramer A. NO fluorescence decay from low-lying electronic states excited into single vibronic levels with synchrotron radiation. Chem Phys 1975;9(3):327–38.

[118] Banic JR, Lipson RH, Stoicheff BP. Vacuum ultraviolet laser spectroscopy: I. Fluorescence studies of the $B'^2\Delta$ state of NO. Can J Phys 1984;62(12):1629–38.

[119] Banic JR, Lipson RH, Efthimiopoulos T, Stoicheff BP. Radiative lifetimes of the $B'^2\Delta$ state ($v'=$ 0-8) of NO obtained by vacuum-ultraviolet laser excitation. Opt Lett 1981;6(10):461–3.

[120] Taherian MR, Slanger TG. Radiative and kinetic properties of NO ($B'^2\Delta$). J Chem Phys 1985;83(10):5349–51.

[121] Yoshino K, Freeman DE, Esmond JR, Friedman RS, Parkinson WH. High resolution absorption cross section measurements and band oscillator strengths of the (1, 0)-(12, 0) Schumann–Runge bands of O_2. Planet Space Sci 1983;31(3):339–53.

[122] Lewis BR, Berzins L, Carver JH. Oscillator strengths for the Schumann–Runge bands of $^{16}O_2$. J Quant Spectrosc Radiat Transfer 1986;36(3):209–32.

[123] Field RW, d'Azy OB, Lavollée M, Lopez-Delgado R, Tramer A. Radiative decay rates from deperturbed v= 0-7 vibrational levels of CO $A^1\Pi$ measured using synchrotron radiation. J Chem Phys 1983;78(6):2838–46.

[124] Sprang HAV, Möhlmann GR, Heer FJD. Radiative lifetimes of the absolute emission $a'^3\Sigma^+$, $b^3\Sigma^+$, $c^3\Pi$, $d^3\Delta$ and $B^1\Sigma^+$ cross sections for $a'^3\Sigma^+ - A^3\Pi$ and $C^3\Pi - A^3\Pi$ transitions for electrons on CO. Chem Phys 1977;24(3):429–33.

[125] Lavendy H, Gandara G, Robbe JM. Oscillator strengths, radiative lifetimes, and photodissociation cross-sections for CN. J Mol Spectrosc 1984;106(2):395–410.

[126] CW Jr Bauschlicher, Langhoff SR, Taylor PR. Theoretical study of the dissociation energy and the red and violet band systems of CN. Astrophys J 1988;332:531–8.

[127] Jeunehomme M. Oscillator strength of the CN red system. J Chem Phys 1965;42(12):4086–8.

[128] Duric N, Erman P, Larsson M. The influence of collisional transfers and perturbations on measured A and B state lifetimes in CN. Phys Scr 1978;18(1):39.

[129] Taherian MR, Slanger TG. C_2N_2 photodissociation at 1576Å. I. CN ($A^2\Pi$) radiative lifetimes, nascent vibrational distribution, and C_2N_2 quenching. J Chem Phys 1984;81(9):3814–19.

[130] O'Neil SV, Rosmus P, Werner HJ. Radiative transition probabilities in the Phillips band system of C_2. J Chem Phys 1987;87:2847.

[131] Erman P, Larsson M, Mannfors B, Lambert DL. Time-resolved spectroscopy of the C_2 Phillips system and revised interstellar C_2 abundances. Astrophys J 1982;253:983–8.

[132] Bauer W, Becker KH, Hubrich C, Meuser R, Wildt J. Radiative lifetime measurements of the C_2 ($A^1\Pi_u$) state. Astrophys J 1985;296:758–64.

[133] Bauer W, Becker KH, Bielefeld M, Meuser R. Lifetime measurements on electronically excited C_2 ($A^1\Pi_u$) and C_2 ($d^3\Pi_g$) by laser-induced fluorescence. Chem Phys Lett 1986;123(1):33–6.

[134] Tatarczyk T, Fink EH, Becker KH. Lifetime measurements on single vibrational levels of C_2 ($d^3\Pi_g$) by laser fluorescence excitation. Chem Phys Lett 1976;40(1):126–30.

[135] Nishi N, Shinohara H, Hanazaki I. VUV laser photofragmentations of an acrylonitrile molecular beam: one-, two- and three-photon processes. J Chem Phys 1982;77(1):246–57.

[136] Naulin C, Costes M, Dorthe G. C_2 Radicals in a supersonic molecular beam. Radiative lifetime of the $d^3\Pi_g$ state measured by laser-induced fluorescence. Chem Phys Lett 1988;143(5):496–500.

[137] Bergström H, Hallstadius H, Lundberg H, Persson A. Detection of carbon using amplified laser-induced fluorescence. Chem Phys Lett 1989;155(1):27–31.

[138] Smith WH. Transition probabilities for the Swan and Mulliken C_2 bands. Astrophys J 1969;156:791.

[139] Möhlmann GR, Heer FJD. Measurements of the radiative lifetimes of the vibrational CO^+ ($A^2\Pi_i$) states. Chem Phys Lett 1976;43(1):170–4.

[140] Mahan BH, Okeefe A. Radiative lifetimes of excited electronic states in molecular ions. Astrophys J 1981;248:1209–16.

[141] Dumont MN, Remy F. Experimental determination of the radiative lifetime of the 0, 1, 2, 3 vibrational levels of the $B^2\Sigma^+$ state in CO^+.. J Quant Spectrosc Radiat Transf 1979;22(2):209–11.

[142] Arqueros F, Campos J. Lifetime of vibrational levels of the $A^2\Pi$ and $B^2\Sigma^+$ states of CO^+. J Chem Phys 1981;74(11):6092–5.

[143] Marian CM, Larsson M, Olsson B J, Sigray P. Theoretical and experimental studies of radiative lifetimes of excited electronic states in CO^+. Chem Phys 1989;130(1-3):361–70.

[144] Fantz U, Wünderlich D. Franck–Condon factors, transition probabilities and radiative lifetimes for hydrogen molecules and their isotopomeres. Atom Data Nucl Data Tables 2006;92(6):853–973.

[145] Rizzo A, Graham RL, Yeager DL. Accurate transition moments between the $A^3\Sigma_u^+$, $B^3\Pi_g$ and $B'^3\Sigma_u^-$ of N_2 using multiconfigurational linear response. J Chem Phys 1988;89(3):1533–9.

[146] Michels HH. Calculation of the integrated band intensities of NO. J Quant Spectrosc Radiat Transf 1971;11(11):1735–9.

[147] Chandraiah G, Cho CW. A study of the fundamental and first overtone bands of NO in NO-rare gas mixtures at pressures up to 10000 PSI. J Mol Spectrosc 1973;47(1):134–47.

[148] King WT, Crawford B. The integrated intensity of the nitric oxide fundamental band. J Quant Spectrosc Radiat Transf 1972;12(3):443–7.

[149] Garside BK, Ballik EA, Elsherbiny M, Shewchun J. Resonance absorption measurements of NO with a line-tunable CO laser: spectroscopic data for pollution monitoring. Appl Optics 1977;16(2):398–402.

[150] Kunimori K, Horiguchi H, Tsuchiya S. Intensity and line-width measurements of the NO fundamental by infrared molecular absorption spectrometry. J Quant Spectrosc Radiat Transf 1978;19(2):127–33.

[151] Holland RF, Vasquez MC, Beattie WH, Mcdowell RS. Absorptivity of nitric oxide in the fundamental vibrational band. J Quant Spectrosc Radiat Transf 1983;29(5):435–8.

[152] Rogers J, Anderson R. Radiative lifetime of the $b^3\Sigma^+$ state of CO. J Quant Spectrosc Radiat Transf 1970;10(5):515–17.

[153] Rogers J, Anderson R. Radiative lifetime of the $B^1\Sigma^+$ state of CO. Josa 1970;60(2):278–9.

[154] Kuznetsova LA, Stepanov NF. Recommendations from the raden data base for the electronic transition moments on diatomic molecules of astrophysical interest. I: C_2, CH and CN molecules. Astron Astrophys Trans 1997;12(4):289–311.

[155] Bauschlicher CWJ, Langhoff SR, Taylor PR. Theoretical study of the dissociation energy and the red and violet band systems of CN. Astrophys J 1988;332(1):531–8.

[156] Cooper DM, Nicholls RW. Transition probability data for seven band systems of C_2. Spectr Lett 1976;9(3):139–55.

[157] Cooper DM. Measurements of the electronic transition moments of C_2-band systems. J Quant Spectrosc Radiat Transf 1975;15(2):139–50.
[158] Stephens TL, Dalgarno A. Spontaneous radiative dissociation in molecular hydrogen. J Quant Spectrosc Radiat Transf 1972;12(4):569–86.
[159] Pardo A. Radiative lifetimes for the $B^1\Sigma_u^+$ state of the H_2 molecule. Spectroc Acta Pt A Molec 1998;54(10):1433–41.
[160] Hesser JE, Dressler K. Radiative lifetimes of ultraviolet molecular transitions. J Chem Phys 1966;45(8):3149–50.
[161] Smith WH, Chevalier R. Radiative-lifetime studies of the emission continua of the hydrogen and deuterium molecules. Astrophys J 1972;177:835.
[162] Schmoranzer H, Imschweiler J. Radiative lifetimes and collisional quenching cross sections of selectively excited vibrational states of the $B^2\Sigma_u^+$ state of H_2. Phys Lett A 1984;100(2):85–7.
[163] Jiang W, Wilson AK. Multireference composite approaches for the accurate study of ground and excited electronic states: C_2, N_2, and O_2. J Chem Phys 2011;134(3):034101.
[164] Shi D, Xing W, Sun J, Zhu Z, Liu Y. Spectroscopic constants and molecular properties of $A^2\Pi_u$ and $D^2\Pi_g$ electronic states of the ion. Comput Theor Chem 2011;966(1):44–53.
[165] Aoto T, Yoshii H, Hayaishi T, Morioka Y. Rotationally resolved ZEKE spectra of the $X^2\Sigma_g^+$ (v^+= 0-3), $B^2\Sigma_u^+$ (v^+= 0) and $C^2\Sigma_u^+$ (v^+= 0) states of N_2^+. Phys Scr 2002;65(2):139.
[166] Okada K, Aoyagi M, Iwata S. Accurate evaluation of Einstein's A and B coefficients of rovibrational transitions for carbon monoxide: Spectral simulation of $\Delta v = 2$ rovibrational transitions in the solar atmosphere observed by a satellite. J Quant Spectrosc Radiat Transf 2002;72(6):813–25.
[167] Reddy RR, Ahammed YN, Gopal K R, Basha DB. Spectroscopic investigations on cometary molecules CO^+, CH and CH^+. J Quant Spectrosc Radiat Transf 2004;85(1):105–13.
[168] Ostrowska-Kopeć M, Piotrowska I, Kępa R, Kowalczyk P, Zachwieja M, Hakalla R. New observations and analyses of highly excited bands of the fourth-positive ($A^1\Pi - X^1\Sigma^+$) band system in $^{12}C^{16}O$. J Mol Spectrosc 2015;314:63–72.
[169] Ram RS, Davis SP, Wallace L, Engleman R, Appadoo DRT, Bernath PF. Fourier transform emission spectroscopy of the $B^2\Sigma^+ - X^2\Sigma^+$ system of CN. J Mol Spectrosc 2006;237(2):225–31.
[170] Boschen JS, Theis D, Ruedenberg K, Windus TL. Accurate ab initio potential energy curves and spectroscopic properties of the four lowest singlet states of C_2. Theor Chem Acc 2014;133(2):1425.
[171] Kulik HJ, Steeves AH, Field RW. Ab initio investigation of high multiplicity $\Sigma^+ - \Sigma^+$ optical transitions in the spectra of CN and isoelectronic species. J Mol Spectrosc 2009;258(1):6–12.
[172] Ni C, Cheng J, Cheng X. Ab initio calculations for the first-positive bands of N_2. J Mol Spectrosc 2017;331:17–22.
[173] Fantz U, Wunderlich D. Franck–Condon factors, transition probabilities and radiative lifetimes for hydrogen molecules and their isotopomeres. INDC (NDS)-457 report 2004.